

*Electronic Supplementary Information*

## **Coordination-induced emission enhancement in copper(I) iodide coordination polymers supported by 2-(alkylsulfanyl)pyrimidines**

Katerina A. Vinogradova,<sup>\*a</sup> Nikita A. Shekhovtsov,<sup>\*a</sup> Alexey S. Berezin,<sup>a</sup> Taisiya S. Sukhikh,<sup>a</sup>  
Maxim I. Rogovoy,<sup>a</sup> Alexander V. Artem'ev<sup>a</sup> and Mark B. Bushuev<sup>\*a</sup>

<sup>a</sup> *Nikolaev Institute of Inorganic Chemistry, Siberian Branch of Russian Academy of Sciences, 3, Acad. Lavrentiev Ave., Novosibirsk, 630090, Russia. E-mail addresses: vinogradova@niic.nsc.ru (Katerina A. Vinogradova), shna1998@mail.ru (Nikita A. Shekhovtsov), bushuev@niic.nsc.ru (Mark B. Bushuev). Fax: +7 383 330 94 89; Tel: +7 383 316 51 43.*

## Table of Contents

Figure S1.....	4
Figure S2.....	5
Figure S3.....	6
Figure S4.....	6
Figure S5.....	6
Table S1.....	7
Table S2.....	8
Table S3.....	10
Table S4.....	13
Table S5.....	16
Table S6.....	20
Table S7.....	20
Figure S6.....	21
Figure S7.....	21
Table S8.....	21
Table S9.....	23
Table S10.....	24
Table S11.....	24
Table S12.....	26
Table S13.....	27
Table S14.....	27
Table S15.....	28
Table S16.....	30
Table S17.....	30
Table S18.....	31
Table S19.....	31
Table S20.....	31
Table S21.....	32
Table S22.....	32
Table S23.....	33
Table S24.....	33
Table S25.....	33
Table S26.....	34
Table S27.....	34
Table S28.....	35

Table S29 .....	35
Figure S8 .....	36
Figure S9 .....	37
Table S30 .....	38
Figure S10 .....	39
Figure S11 .....	39
Table S31 .....	40
Figure S12 .....	41
Figure S13 .....	41
Table S32 .....	42
Figure S14 .....	43
Figure S15 .....	43
Figure S16 .....	44
Figure S17 .....	44
Figure S18 .....	44
Figure S19 .....	45
Figure S20 .....	46
Figure S21 .....	47
Figure S22 .....	48

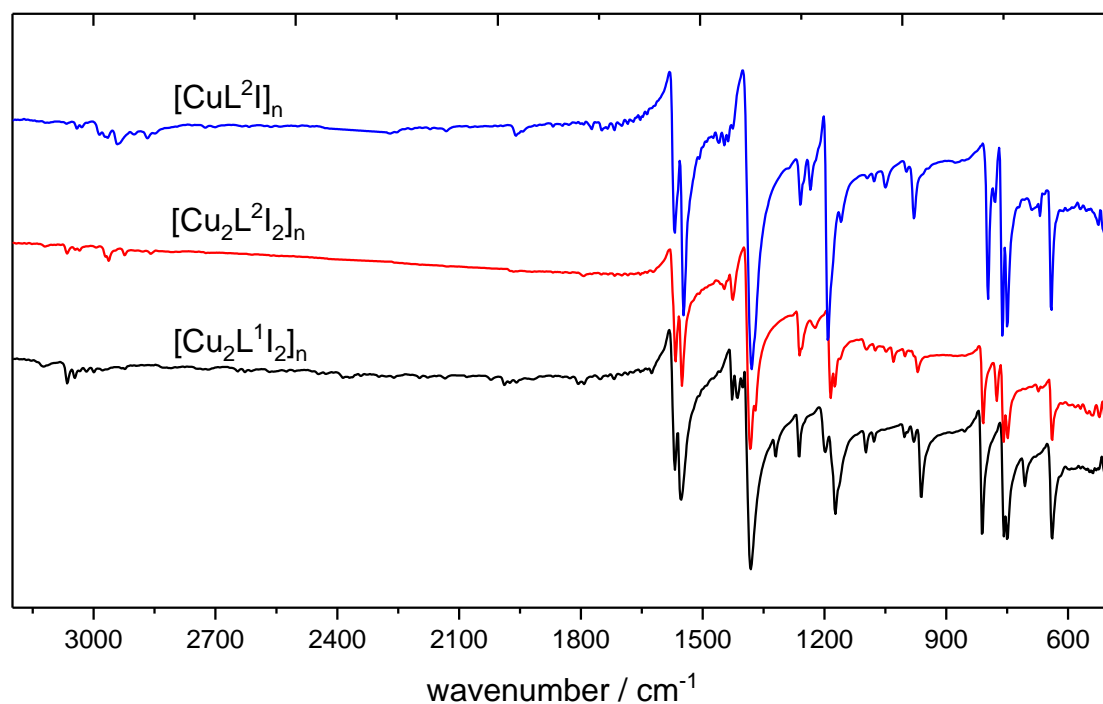


Figure S1. IR spectra of the complexes.

In the region  $3100 - 2850 \text{ cm}^{-1}$ , weak bands to the left of  $3000 \text{ cm}^{-1}$  can be attributed to  $\nu(\text{C-H})$  vibrations of the pyrimidine ring, whereas those to the left of  $3000 \text{ cm}^{-1}$  belong to  $\nu(\text{C-H})$  vibrations of the alkyl groups. Intense bands in the  $1570 - 1545 \text{ cm}^{-1}$  range can be assigned to the stretching vibrations of the pyrimidine ring.<sup>S1</sup> Although it is difficult to assign bands in the fingerprint region ( $1450 \text{ cm}^{-1}$  and below, C-C and C-S stretching vibrations and deformation vibrations of various groups), a weak band at  $1320 \text{ cm}^{-1}$  in the spectrum of  $[\text{Cu}_2\text{L}^1\text{I}_2]_n$ , which is absent in the spectrum of the complexes with  $\text{L}^2$ , is informative of the  $\nu(\text{S-CH}_3)$  vibrations.<sup>S2</sup>

S1 S. Breda, I.D. Reva, L. Lapinski, M.J. Nowak and R. Fausto, *J. Mol. Struct.*, 2006, **786**, 193–206.

S2 K. Nakanishi, *Infrared Absorption Spectroscopy*, Holden-Day, Inc., San Francisco and Nankodo Company limited, Tokyo, 1962.

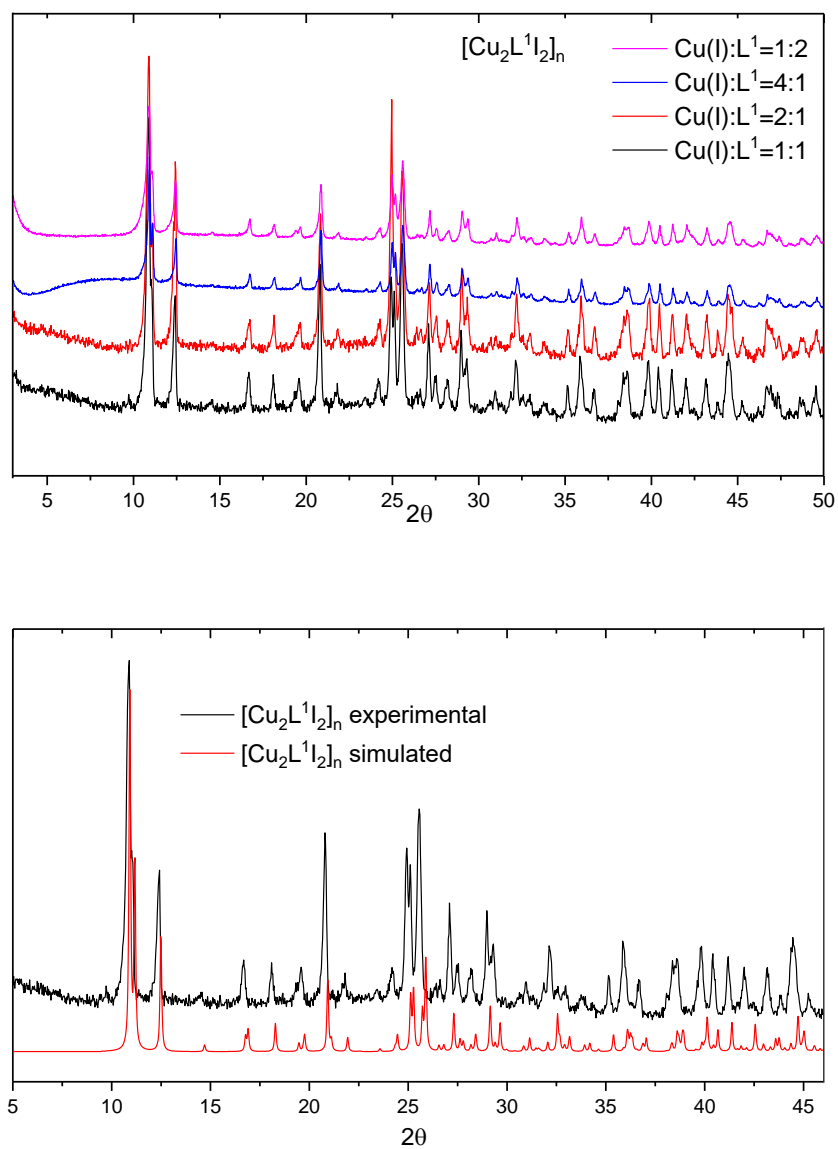


Figure S2. X-ray powder diffraction patterns of  $[\text{Cu}_2\text{L}^1\text{I}_2]_n$ .

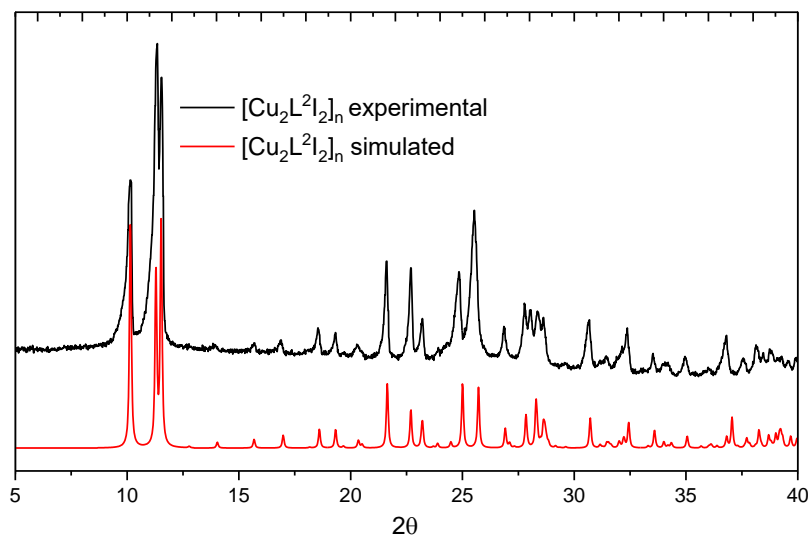


Figure S3. X-ray powder diffraction patterns of  $[\text{Cu}_2\text{L}^2\text{I}_2]_n$ .

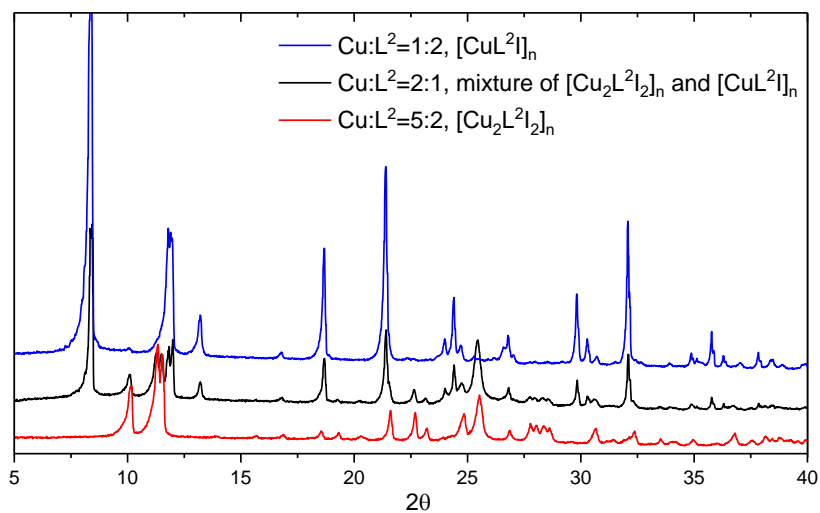


Figure S4. X-ray powder diffraction patterns of  $[\text{Cu}_2\text{L}^2\text{I}_2]_n$ ,  $[\text{CuL}^2\text{I}]_n$  and their mixture.

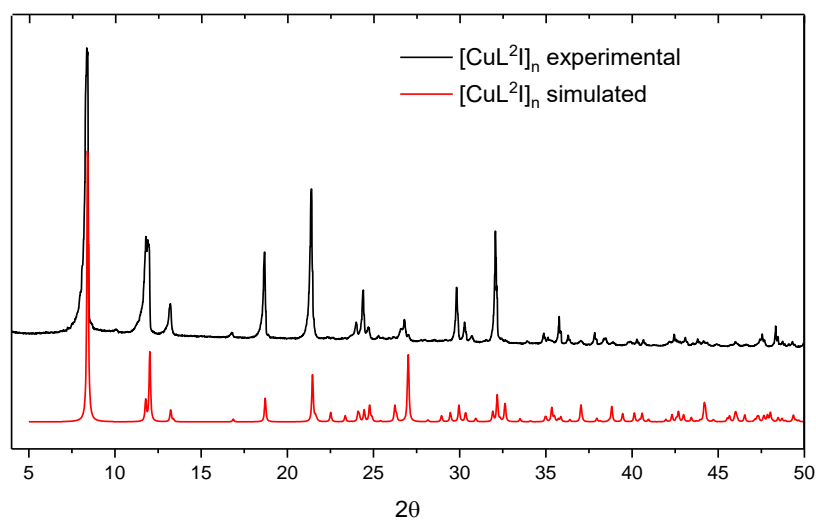


Figure S5. X-ray powder diffraction patterns of  $[\text{CuL}^2\text{I}]_n$ .

Table S1. Crystallographic data of the complexes  $[\text{Cu}_2\text{L}^1\text{I}_2]_n$ ,  $[\text{Cu}_2\text{L}^2\text{I}_2]_n$  and  $[\text{CuL}^2\text{I}]_n$ .

Identification code	$[\text{Cu}_2\text{L}^1\text{I}_2]_n$	$[\text{Cu}_2\text{L}^2\text{I}_2]_n$	$[\text{CuL}^2\text{I}]_n$
Empirical formula	$\text{C}_5\text{H}_6\text{Cu}_2\text{I}_2\text{N}_2\text{S}$	$\text{C}_6\text{H}_8\text{Cu}_2\text{I}_2\text{N}_2\text{S}$	$\text{C}_6\text{H}_8\text{CuIN}_2\text{S}$
Formula weight	507.06	521.08	330.64
Space group	$P\bar{1}$	$P\bar{1}$	$P2_1/c$
a/Å	7.6410(4)	7.5758(6)	4.1293(4)
b/Å	8.5752(4)	9.4445(9)	15.0107(13)
c/Å	9.4222(5)	9.9008(8)	14.8554(13)
$\alpha/^\circ$	67.325(2)	61.958(3)	90
$\beta/^\circ$	67.177(2)	82.979(3)	97.948(3)
$\gamma/^\circ$	81.785(2)	66.443(2)	90
Volume/Å <sup>3</sup>	525.04(5)	571.24(9)	911.95(14)
Z	2	2	4
$\rho_{\text{calc}}/\text{cm}^3$	3.207	3.029	2.408
$\mu/\text{mm}^{-1}$	10.076	9.266	5.946
F(000)	460.0	476.0	624.0
Crystal size/mm <sup>3</sup>	0.35 × 0.29 × 0.1	0.13 × 0.12 × 0.12	0.28 × 0.05 × 0.05
2 $\theta$ range for data collection/ $^\circ$	5.148 to 54.42	4.676 to 54.456	2.714 to 56.208
Index ranges	$-9 \leq h \leq 9, -9 \leq k \leq 10, -12 \leq l \leq 12$	$-9 \leq h \leq 9, -12 \leq k \leq 9, -12 \leq l \leq 11$	$-4 \leq h \leq 5, -19 \leq k \leq 19, -19 \leq l \leq 12$
Reflections collected	6767	5668	10024
Independent reflections	2317 [ $R_{\text{int}} = 0.0283, R_{\text{sigma}} = 0.0280$ ]	2468 [ $R_{\text{int}} = 0.0207, R_{\text{sigma}} = 0.0275$ ]	2167 [ $R_{\text{int}} = 0.0320, R_{\text{sigma}} = 0.0257$ ]
Restraints/parameters	0/110	0/119	0/102
Goodness-of-fit on $F^2$	1.245	1.072	1.055
Final R indexes [ $I \geq 2\sigma(I)$ ]	$R_1 = 0.0215, wR_2 = 0.0538$	$R_1 = 0.0203, wR_2 = 0.0404$	$R_1 = 0.0190, wR_2 = 0.0461$
Final R indexes [all data]	$R_1 = 0.0221, wR_2 = 0.0541$	$R_1 = 0.0229, wR_2 = 0.0415$	$R_1 = 0.0196, wR_2 = 0.0464$
Largest diff. peak/hole / e Å <sup>-3</sup>	0.72/-1.48	0.60/-0.66	1.28/-0.47

**Table S2.** A search of CCDC structures (CSD version 5.41, Mar 2020) containing  $(\text{Cu}_2\text{I})_n$  ribbons. Dihedral angles between  $\{\text{Cu}_2\text{I}\}$  planes (deg.) as well as Cu–I and Cu...Cu distances (Å) in  $\{\text{Cu}_2\text{I}_2\}$  quadrangles and ligand type are listed. *m* is for supporting ligands that do not bind Cu atoms in a ribbon; *b* is for ligands that bridge Cu atoms in a ribbon. Note that bridging ligands connecting only adjacent ribbons are assigned *m*-type. The cases where ligand type is *m*, but the dihedral angle is far from 180°, are highlighted yellow.



Queries used were:  $\text{Cu} - \text{I} - \text{Cu} - \text{I}$  ,  $\text{Cu} - \text{I} - \text{Cu} - \text{I}$  ,

ignoring structures with further coordination Cu and I atoms (e.g. cubane-like structures and triple ribbons). The total number of structures ignoring retaken ones was 47. Most of them present almost flat  $\{\text{Cu}_2\text{I}_2\}$  quadrangles with the dihedral angle greater than 175°. 14 structures reveal both flat (>175°) and folded (<175°)  $\{\text{Cu}_2\text{I}_2\}$  fragments, while 3 structures (viz. DIVKUQ, DUFHAP and RUPTED) exhibit only folded fragments. Cu–I bonds range from 2.56 to 2.88 Å, while Cu...Cu distances range from 2.61 to 3.76 Å; no correlation between these distances and the dihedral angle was found. No correlation between Cu...Cu distance and ligand type was also found.

Index	Refcode	ligand type	dihedral angle	Cu–I	Cu...Cu	Index	Refcode	ligand type	dihedral angle	Cu–I	Cu...Cu
1	ACIGAX	<i>m</i>	180.00	2.73	3.21	64	MRHCUI	<i>m</i>	180.00	2.67	2.96
2	ACIGAX	<i>m</i>	180.00	2.73	2.92	65	MUHQOV	<i>m</i>	180.00	2.73	3.41
3	AGIYEU01	<i>m</i>	180.00	2.65	2.76	66	MUHQOV	<i>m</i>	180.00	2.64	2.78
4	AGIYEU01	<i>m</i>	180.00	2.61	2.76	67	MUHQOV01	<i>m</i>	180.00	2.67	2.80
5	AGIYEU02	<i>m</i>	180.00	2.66	2.79	68	MUHQOV01	<i>m</i>	180.00	2.74	3.41
6	AYELOH	<i>m</i>	180.00	2.56	2.75	69	NEKXAD	<i>m</i>	180.00	2.69	3.33
7	AYELOH	<i>m</i>	180.00	2.76	2.87	70	OMIHEX	<i>m</i>	179.30	2.64	2.85
8	AYELOH	<i>m</i>	175.77	2.71	3.12	71	ONAXUX	<i>b</i>	180.00	2.76	3.52
9	BIGLUY	<i>b</i>	180.00	2.59	2.62	72	ONAXUX	<i>b</i>	155.60	2.76	3.52
10	BIGLUY	<i>b</i>	180.00	2.58	2.61	73	ORUSAW	<i>m</i>	180.00	2.67	3.36
11	BIGLUY	<i>b</i>	131.43	2.74	2.76	74	ORUSAW	<i>m</i>	180.00	2.67	2.76
12	BUWJIN	<i>b</i>	180.00	2.71	3.32	75	QALNOJ	<i>m</i>	180.00	2.66	2.69
13	BUWJIN	<i>b</i>	180.00	2.70	3.76	76	QALNOJ	<i>m</i>	180.00	2.61	3.00
14	BUWJIN	<i>b</i>	164.17	2.71	3.55	77	QEZBEF	<i>b</i>	180.00	2.62	2.79
15	CAJQOT	<i>m</i>	180.00	2.63	3.44	78	QEZBEF	<i>b</i>	145.81	2.62	2.79
16	CAJQOT	<i>m</i>	180.00	2.77	2.89	79	REJCAL	<i>b</i>	180.00	2.68	2.80
17	CAJQOT	<i>m</i>	172.03	2.68	2.92	80	REJCAL	<i>b</i>	164.96	2.68	2.80
18	CEPFOS	<i>m</i>	180.00	2.65	2.65	81	RIWXIF	<i>b</i>	180.00	2.69	2.64
19	CEPFOS	<i>m</i>	180.00	2.74	3.56	82	RIWXIF	<i>b</i>	180.00	2.63	2.72
20	CEZBEQ	<i>m</i>	180.00	2.63	2.77	83	RIWXIF	<i>b</i>	145.62	2.69	2.88
21	CEZBEQ	<i>m</i>	180.00	2.68	2.73	84	RUPTED	<i>m</i>	158.25	2.66	2.69
22	CUIPYS	<i>m</i>	179.27	2.64	2.87	85	RUPTED	<i>m</i>	157.41	2.66	2.69
23	DIVKUQ	<i>m</i>	150.43	2.69	2.94	86	SAWTOZ	<i>m</i>	180.00	2.77	2.91
24	DIVKUQ	<i>m</i>	144.60	2.63	2.80	87	TAWKUZ	<i>b</i>	180.00	2.67	2.72
25	DUFHAP	<i>b</i>	151.32	2.64	2.81	88	TAWKUZ	<i>b</i>	180.00	2.62	2.76
26	DUFHAP	<i>b</i>	137.62	2.65	2.64	89	TAWKUZ	<i>b</i>	137.05	2.72	2.84
27	ECEVIS	<i>m</i>	180.00	2.74	3.54	90	TIYZOT	<i>b</i>	180.00	2.67	2.78
28	ECEVIS	<i>m</i>	180.00	2.66	3.08	91	TIYZOT	<i>b</i>	180.00	2.71	3.65
29	ECEVIS	<i>m</i>	170.52	2.65	2.86	92	TIYZOT	<i>b</i>	163.86	2.67	2.78



30	FALYEW	<i>m</i>	180.00	2.68	2.71	93	TIYZOT	<i>b</i>	162.50	2.71	3.65
31	FALYIA	<i>m</i>	180.00	2.78	3.60	94	TIYZOT01	<i>b</i>	180.00	2.67	2.73
32	FOLBAJ	<i>m</i>	180.00	2.74	2.96	95	TIYZOT01	<i>b</i>	165.64	2.70	3.63
33	GUYQAU	<i>m</i>	179.62	2.70	3.13	96	TIYZOT01	<i>b</i>	162.76	2.70	3.63
34	GUYQAU	<i>m</i>	179.41	2.71	3.21	97	TOKGAB	<i>m</i>	179.70	2.65	2.90
35	HALZAW	<i>m</i>	180.00	2.68	2.93	98	VEVGUY	<i>m</i>	179.36	2.76	3.51
36	HALZAW	<i>m</i>	178.48	2.66	2.96	99	VEVGUY	<i>m</i>	177.91	2.70	2.79
37	HUJHID	<i>m</i>	179.97	2.67	2.82	100	VEYJUE	<i>m</i>	180.00	2.71	3.21
38	HUJHUP	<i>m</i>	180.00	2.63	2.70	101	VIXBEK	<i>m</i>	178.10	2.75	2.83
39	HUJHUP	<i>m</i>	180.00	2.69	2.76	102	WEMDAU	<i>m</i>	180.00	2.74	3.17
40	HUJHUP01	<i>m</i>	180.00	2.63	2.72	103	XAKNED	<i>m</i>	180.00	2.61	2.73
41	HUJHUP01	<i>m</i>	180.00	2.69	2.78	104	XAKNED	<i>m</i>	180.00	2.61	2.65
42	JULWOE	<i>m</i>	179.27	2.62	3.17	105	XAKNED	<i>m</i>	180.00	2.65	3.03
43	JULWOE	<i>m</i>	179.17	2.69	2.80	106	XAKNED	<i>m</i>	167.89	2.76	3.19
44	KALNOA	<i>m</i>	180.00	2.68	2.82	107	XIHFAV	<i>m</i>	180.00	2.66	2.86
45	KAWGOG	<i>b</i>	180.00	2.69	2.91	108	XIHFAV	<i>m</i>	180.00	2.66	2.87
46	KAWGOG	<i>b</i>	180.00	2.71	2.90	109	ZEBNUP	<i>m</i>	180.00	2.63	2.85
47	KAWGOG	<i>b</i>	153.76	2.69	2.91	110	ZEBNUP	<i>m</i>	180.00	2.65	2.78
48	KAWGOG	<i>b</i>	145.23	2.71	2.90	111	ZEBNUP	<i>m</i>	177.48	2.62	2.77
49	LAGVAS	<i>m</i>	178.80	2.61	2.79	112	ZGRIM01	<i>m</i>	180.00	2.66	3.12
50	LAGVAS	<i>m</i>	178.47	2.66	3.00	113	ZGRIM02	<i>m</i>	180.00	2.65	3.01
51	LIGGOA	<i>b</i>	180.00	2.65	3.43	114	ZGRIM03	<i>m</i>	180.00	2.64	3.01
52	LIGGOA	<i>b</i>	152.71	2.72	2.72	115	ZGRIM10	<i>m</i>	178.95	2.64	3.02
53	LUZQAA	<i>b</i>	180.00	2.67	2.84						
54	LUZQAA	<i>b</i>	180.00	2.67	2.94						
55	LUZQAA	<i>b</i>	179.89	2.61	3.12						
56	LUZQAA	<i>b</i>	179.02	2.70	3.15						
57	LUZQAA	<i>b</i>	178.58	2.60	3.01						
58	LUZQAA	<i>b</i>	174.87	2.67	2.92						
59	LUZQAA	<i>b</i>	174.58	2.88	3.63						
60	LUZQAA	<i>b</i>	174.30	2.71	3.65						
61	LUZQAA	<i>b</i>	171.15	2.85	3.67						
62	LUZQAA	<i>b</i>	170.90	2.62	3.73						
63	LUZQAA	<i>b</i>	169.04	2.73	3.72						

**Table S3.** Gas phase geometries of the model  $\{\text{Cu}_8\text{I}_8(\text{L}^1)_4\}$  (the complex  $[\text{Cu}_2\text{L}^1\text{I}_2]_n$ ) in Cartesian (XYZ) coordinates as calculated in Gaussian software at the B3LYP/LANL2DZ/D95V level of theory.

Ground state ( $S_0$ )			
I	2.808719000000	-0.803896000000	-1.891077000000
I	0.837818000000	2.158802000000	0.252364000000
Cu	1.219430000000	-0.540472000000	0.240286000000
Cu	3.260402000000	1.225282000000	-0.185623000000
S	4.665610000000	3.162936000000	-1.325631000000
N	6.738097000000	1.514641000000	-1.963886000000
N	5.974790000000	2.963160000000	-3.726397000000
C	7.703015000000	1.023720000000	-2.792997000000
H	8.330850000000	0.238410000000	-2.385906000000
C	5.911811000000	2.482949000000	-2.469335000000
C	3.576232000000	4.136041000000	-2.519690000000
H	3.187305000000	3.459566000000	-3.280961000000
H	2.767021000000	4.530080000000	-1.901452000000
H	4.163677000000	4.933857000000	-2.972279000000
C	7.846067000000	1.487941000000	-4.108408000000
H	8.613596000000	1.090680000000	-4.761261000000
C	6.936858000000	2.468284000000	-4.543544000000
H	6.964559000000	2.869369000000	-5.552277000000
I	4.832268000000	0.803919000000	1.891108000000
I	-0.837818000000	-2.158802000000	-0.252364000000
Cu	-1.219430000000	0.540472000000	-0.240286000000
Cu	6.421260000000	0.540928000000	-0.240070000000
Cu	4.380865000000	-1.225647000000	0.185439000000
N	1.538437000000	-1.020321000000	2.280844000000
I	-4.832268000000	-0.803919000000	-1.891108000000
I	-6.803113000000	2.158722000000	0.252355000000
Cu	-6.421260000000	-0.540928000000	0.240070000000
Cu	-4.380865000000	1.225647000000	-0.185439000000
S	-3.116315000000	3.061879000000	-1.457647000000
N	-1.538437000000	1.020321000000	-2.280844000000
N	-2.438739000000	2.406199000000	-4.032321000000
C	-0.900594000000	0.263807000000	-3.214179000000
H	-0.316703000000	-0.569525000000	-2.842096000000
C	-2.281287000000	2.067833000000	-2.738295000000
C	-4.365591000000	4.015587000000	-2.501714000000
H	-4.978750000000	3.308745000000	-3.060818000000
H	-4.975451000000	4.562599000000	-1.780144000000
H	-3.829955000000	4.685927000000	-3.172989000000
C	-1.009319000000	0.543676000000	-4.585922000000
H	-0.502770000000	-0.070080000000	-5.320879000000
C	-1.806021000000	1.639276000000	-4.956180000000
H	-1.950665000000	1.921160000000	-5.995013000000
I	-2.808719000000	0.803896000000	1.891077000000
Cu	-3.260402000000	-1.225282000000	0.185623000000
N	-6.738097000000	-1.514641000000	1.963886000000
I	6.803113000000	-2.158722000000	-0.252355000000
S	3.116315000000	-3.061879000000	1.457647000000
N	2.438739000000	-2.406199000000	4.032321000000
C	0.900594000000	-0.263807000000	3.214179000000
H	0.316703000000	0.569525000000	2.842096000000

C	2.281287000000	-2.067833000000	2.738295000000
C	4.365591000000	-4.015587000000	2.501714000000
H	4.978750000000	-3.308745000000	3.060818000000
H	4.975451000000	-4.562599000000	1.780144000000
H	3.829955000000	-4.685927000000	3.172989000000
C	1.009319000000	-0.543676000000	4.585922000000
H	0.502770000000	0.070080000000	5.320879000000
C	1.806021000000	-1.639276000000	4.956180000000
H	1.950665000000	-1.921160000000	5.995013000000
S	-4.665610000000	-3.162936000000	1.325631000000
N	-5.974790000000	-2.963160000000	3.726397000000
C	-7.703015000000	-1.023720000000	2.792997000000
H	-8.330850000000	-0.238410000000	2.385906000000
C	-5.911811000000	-2.482949000000	2.469335000000
C	-3.576232000000	-4.136041000000	2.519690000000
H	-3.187305000000	-3.459566000000	3.280961000000
H	-2.767021000000	-4.530080000000	1.901452000000
H	-4.163677000000	-4.933857000000	2.972279000000
C	-7.846067000000	-1.487941000000	4.108408000000
H	-8.613596000000	-1.090680000000	4.761261000000
C	-6.936858000000	-2.468284000000	4.543544000000
H	-6.964559000000	-2.869369000000	5.552277000000

**Lowest triplet excited state (T<sub>1</sub>)**

I	2.808706000000	-0.803886000000	-1.891076000000
I	0.837759000000	2.158861000000	0.252369000000
Cu	1.219297000000	-0.540188000000	0.240481000000
Cu	3.260554000000	1.225102000000	-0.185698000000
S	4.577153000000	3.172531000000	-1.238175000000
N	6.769264000000	1.637794000000	-1.848842000000
N	6.041602000000	3.192609000000	-3.543989000000
C	7.838627000000	1.277917000000	-2.664166000000
H	8.498273000000	0.510597000000	-2.275914000000
C	5.935757000000	2.606197000000	-2.357352000000
C	3.476223000000	4.085360000000	-2.466595000000
H	3.095762000000	3.378255000000	-3.204503000000
H	2.663888000000	4.508877000000	-1.872393000000
H	4.070757000000	4.858945000000	-2.949967000000
C	8.024740000000	1.857165000000	-3.919775000000
H	8.861056000000	1.560996000000	-4.543393000000
C	7.091677000000	2.821769000000	-4.355688000000
H	7.154060000000	3.308834000000	-5.321981000000
I	4.832270000000	0.803911000000	1.891124000000
I	-0.837759000000	-2.158861000000	-0.252369000000
Cu	-1.219297000000	0.540188000000	-0.240481000000
Cu	6.421194000000	0.541050000000	-0.239991000000
Cu	4.380890000000	-1.225764000000	0.185286000000
N	1.518847000000	-1.024467000000	2.264765000000
I	-4.832270000000	-0.803911000000	-1.891124000000
I	-6.803108000000	2.158718000000	0.252345000000
Cu	-6.421194000000	-0.541050000000	0.239991000000
Cu	-4.380890000000	1.225764000000	-0.185286000000
S	-3.081664000000	3.070787000000	-1.414423000000
N	-1.518847000000	1.024467000000	-2.264765000000

N	-2.420486000000	2.436359000000	-3.995544000000
C	-0.892322000000	0.271451000000	-3.217284000000
H	-0.314525000000	-0.572864000000	-2.862576000000
C	-2.257746000000	2.083327000000	-2.711287000000
C	-4.310116000000	4.068938000000	-2.441872000000
H	-4.936093000000	3.385588000000	-3.015414000000
H	-4.908375000000	4.617098000000	-1.711619000000
H	-3.757020000000	4.738462000000	-3.099385000000
C	-1.007736000000	0.569893000000	-4.582261000000
H	-0.509238000000	-0.038254000000	-5.327576000000
C	-1.797240000000	1.677396000000	-4.938316000000
H	-1.944837000000	1.975142000000	-5.971659000000
I	-2.808706000000	0.803886000000	1.891076000000
Cu	-3.260554000000	-1.225102000000	0.185698000000
N	-6.769264000000	-1.637794000000	1.848842000000
I	6.803108000000	-2.158718000000	-0.252345000000
S	3.081664000000	-3.070787000000	1.414423000000
N	2.420486000000	-2.436359000000	3.995544000000
C	0.892322000000	-0.271451000000	3.217284000000
H	0.314525000000	0.572864000000	2.862576000000
C	2.257746000000	-2.083327000000	2.711287000000
C	4.310116000000	-4.068938000000	2.441872000000
H	4.936093000000	-3.385588000000	3.015414000000
H	4.908375000000	-4.617098000000	1.711619000000
H	3.757020000000	-4.738462000000	3.099385000000
C	1.007736000000	-0.569893000000	4.582261000000
H	0.509238000000	0.038254000000	5.327576000000
C	1.797240000000	-1.677396000000	4.938316000000
H	1.944837000000	-1.975142000000	5.971659000000
S	-4.577153000000	-3.172531000000	1.238175000000
N	-6.041602000000	-3.192609000000	3.543989000000
C	-7.838627000000	-1.277917000000	2.664166000000
H	-8.498273000000	-0.510597000000	2.275914000000
C	-5.935757000000	-2.606197000000	2.357352000000
C	-3.476223000000	-4.085360000000	2.466595000000
H	-3.095762000000	-3.378255000000	3.204503000000
H	-2.663888000000	-4.508877000000	1.872393000000
H	-4.070757000000	-4.858945000000	2.949967000000
C	-8.024740000000	-1.857165000000	3.919775000000
H	-8.861056000000	-1.560996000000	4.543393000000
C	-7.091677000000	-2.821769000000	4.355688000000
H	-7.154060000000	-3.308834000000	5.321981000000

**Table S4.** Gas phase geometries of the model  $\{\text{Cu}_8\text{I}_8(\text{L}^2)_4\}$  (the complex  $[\text{Cu}_2\text{L}^2\text{I}_2]_n$ ) in Cartesian (XYZ) coordinates as calculated in Gaussian software at the B3LYP/LANL2DZ/D95V level of theory.

<b>Ground state (<math>S_0</math>)</b>			
I	2.793787000000	-2.062865000000	0.081749000000
I	6.745856000000	-1.112760000000	-1.893680000000
Cu	4.321186000000	-0.328140000000	-1.223724000000
Cu	1.217530000000	-0.000683000000	-0.570164000000
S	3.027339000000	0.042648000000	-3.406870000000
N	1.513510000000	1.663041000000	-1.854901000000
N	2.324687000000	2.656615000000	-3.890879000000
C	2.211640000000	1.630129000000	-3.026252000000
C	1.700791000000	3.817202000000	-3.567040000000
H	1.811373000000	4.635737000000	-4.272414000000
C	0.952829000000	3.948479000000	-2.385768000000
H	0.452783000000	4.873245000000	-2.124368000000
C	4.271390000000	0.554694000000	-4.768650000000
H	3.762221000000	1.320995000000	-5.355354000000
H	5.130254000000	0.988966000000	-4.251554000000
C	0.881453000000	2.826386000000	-1.544644000000
H	0.328203000000	2.840999000000	-0.613193000000
C	4.653929000000	-0.682169000000	-5.587224000000
H	5.372757000000	-0.386564000000	-6.363033000000
H	3.779600000000	-1.124622000000	-6.078967000000
H	5.132991000000	-1.445401000000	-4.963843000000
I	4.782010000000	2.062866000000	-0.081757000000
I	-0.829916000000	-1.112773000000	-1.893700000000
I	0.829916000000	1.112773000000	1.893700000000
Cu	3.254678000000	0.328034000000	1.223644000000
Cu	-1.217530000000	0.000683000000	0.570164000000
Cu	6.358201000000	0.000825000000	0.570285000000
I	-4.782010000000	-2.062866000000	0.081757000000
Cu	-3.254678000000	-0.328034000000	-1.223644000000
Cu	-6.358201000000	-0.000825000000	-0.570285000000
S	-4.701002000000	-0.154619000000	-3.437982000000
N	-6.703002000000	1.169041000000	-2.157713000000
N	-6.026229000000	2.112167000000	-4.262388000000
C	-5.922397000000	1.191783000000	-3.283770000000
C	-6.972768000000	3.073135000000	-4.131231000000
H	-7.032327000000	3.802768000000	-4.933414000000
C	-7.828192000000	3.123751000000	-3.016323000000
H	-8.581430000000	3.894638000000	-2.908250000000
C	-3.630961000000	0.436578000000	-4.913245000000
H	-4.304260000000	1.011663000000	-5.550676000000
H	-2.867502000000	1.095085000000	-4.491935000000
C	-7.651756000000	2.139961000000	-2.033023000000
H	-8.240583000000	2.120245000000	-1.121911000000
C	-3.024455000000	-0.783507000000	-5.613889000000
H	-2.400567000000	-0.439670000000	-6.449652000000
H	-3.802794000000	-1.442870000000	-6.014625000000
H	-2.385184000000	-1.362957000000	-4.938803000000
I	-2.793787000000	2.062865000000	-0.081749000000
I	-6.745856000000	1.112760000000	1.893680000000
Cu	-4.321186000000	0.328140000000	1.223724000000

S	4.701002000000	0.154619000000	3.437982000000
N	6.703002000000	-1.169041000000	2.157713000000
N	6.026229000000	-2.112167000000	4.262388000000
C	5.922397000000	-1.191783000000	3.283770000000
C	6.972768000000	-3.073135000000	4.131231000000
H	7.032327000000	-3.802768000000	4.933414000000
C	7.828192000000	-3.123751000000	3.016323000000
H	8.581430000000	-3.894638000000	2.908250000000
C	3.630961000000	-0.436578000000	4.913245000000
H	4.304260000000	-1.011663000000	5.550676000000
H	2.867502000000	-1.095085000000	4.491935000000
C	7.651756000000	-2.139961000000	2.033023000000
H	8.240583000000	-2.120245000000	1.121911000000
C	3.024455000000	0.783507000000	5.613889000000
H	2.400567000000	0.439670000000	6.449652000000
H	3.802794000000	1.442870000000	6.014625000000
H	2.385184000000	1.362957000000	4.938803000000
S	-3.027339000000	-0.042648000000	3.406870000000
N	-1.513510000000	-1.663041000000	1.854901000000
N	-2.324687000000	-2.656615000000	3.890879000000
C	-2.211640000000	-1.630129000000	3.026252000000
C	-1.700791000000	-3.817202000000	3.567040000000
H	-1.811373000000	-4.635737000000	4.272414000000
C	-0.952829000000	-3.948479000000	2.385768000000
H	-0.452783000000	-4.873245000000	2.124368000000
C	-4.271390000000	-0.554694000000	4.768650000000
H	-3.762221000000	-1.320995000000	5.355354000000
H	-5.130254000000	-0.988966000000	4.251554000000
C	-0.881453000000	-2.826386000000	1.544644000000
H	-0.328203000000	-2.840999000000	0.613193000000
C	-4.653929000000	0.682169000000	5.587224000000
H	-5.372757000000	0.386564000000	6.363033000000
H	-3.779600000000	1.124622000000	6.078967000000
H	-5.132991000000	1.445401000000	4.963843000000

**Lowest triplet excited state ( $T_1$ )**

I	3.360846000000	-0.777386000000	1.724025000000
Cu	2.825409000000	1.171670000000	-0.142291000000
S	4.730224000000	2.017481000000	-2.665773000000
C	4.244500000000	3.427047000000	1.048110000000
H	3.617410000000	3.134376000000	1.882413000000
N	4.108477000000	2.686199000000	-0.116378000000
C	5.157881000000	4.482706000000	1.130769000000
H	5.261997000000	5.052625000000	2.047738000000
N	5.814228000000	4.035417000000	-1.161595000000
C	4.922637000000	3.039695000000	-1.166235000000
C	5.939086000000	4.773781000000	-0.005087000000
H	6.669886000000	5.575094000000	-0.022225000000
C	6.018990000000	2.065357000000	-5.156071000000
H	5.040786000000	2.147728000000	-5.645104000000
H	6.260949000000	1.001232000000	-5.044103000000
H	6.768233000000	2.512528000000	-5.822444000000
C	6.039641000000	2.795809000000	-3.807688000000
H	5.789880000000	3.854480000000	-3.901491000000

H	7.002165000000	2.709665000000	-3.298840000000
I	0.768590000000	0.777198000000	-1.724116000000
Cu	1.303755000000	-1.171738000000	0.142445000000
I	-0.768590000000	-0.777198000000	1.724116000000
Cu	-1.303755000000	1.171738000000	-0.142445000000
S	0.090415000000	4.261403000000	0.194199000000
C	-3.048691000000	2.448864000000	1.858007000000
H	-3.483387000000	1.459536000000	1.766570000000
N	-1.935107000000	2.699829000000	1.103844000000
C	-3.604477000000	3.422202000000	2.696621000000
H	-4.488365000000	3.211554000000	3.286685000000
N	-1.861298000000	4.938988000000	1.989645000000
C	-1.383651000000	3.951000000000	1.204739000000
C	-2.969363000000	4.677641000000	2.733740000000
H	-3.334109000000	5.489799000000	3.355321000000
C	1.599754000000	6.573179000000	-0.268940000000
H	1.377982000000	6.483812000000	-1.339097000000
H	2.514573000000	6.006993000000	-0.057586000000
H	1.799891000000	7.630697000000	-0.052156000000
C	0.423557000000	6.095450000000	0.591851000000
H	-0.498835000000	6.639769000000	0.379451000000
H	0.631006000000	6.164294000000	1.661928000000
I	-3.360846000000	0.777386000000	-1.724025000000
Cu	-2.825409000000	-1.171670000000	0.142291000000
S	-4.730224000000	-2.017481000000	2.665773000000
C	-4.244500000000	-3.427047000000	-1.048110000000
H	-3.617410000000	-3.134376000000	-1.882413000000
N	-4.108477000000	-2.686199000000	0.116378000000
C	-5.157881000000	-4.482706000000	-1.130769000000
H	-5.261997000000	-5.052625000000	-2.047738000000
N	-5.814228000000	-4.035417000000	1.161595000000
C	-4.922637000000	-3.039695000000	1.166235000000
C	-5.939086000000	-4.773781000000	0.005087000000
H	-6.669886000000	-5.575094000000	0.022225000000
C	-6.018990000000	-2.065357000000	5.156071000000
H	-5.040786000000	-2.147728000000	5.645104000000
H	-6.260949000000	-1.001232000000	5.044103000000
H	-6.768233000000	-2.512528000000	5.822444000000
C	-6.039641000000	-2.795809000000	3.807688000000
H	-5.789880000000	-3.854480000000	3.901491000000
H	-7.002165000000	-2.709665000000	3.298840000000
S	-0.090415000000	-4.261403000000	-0.194199000000
C	3.048691000000	-2.448864000000	-1.858007000000
H	3.483387000000	-1.459536000000	-1.766570000000
N	1.935107000000	-2.699829000000	-1.103844000000
C	3.604477000000	-3.422202000000	-2.696621000000
H	4.488365000000	-3.211554000000	-3.286685000000
N	1.861298000000	-4.938988000000	-1.989645000000
C	1.383651000000	-3.951000000000	-1.204739000000
C	2.969363000000	-4.677641000000	-2.733740000000
H	3.334109000000	-5.489799000000	-3.355321000000
C	-1.599754000000	-6.573179000000	0.268940000000
H	-1.377982000000	-6.483812000000	1.339097000000
H	-2.514573000000	-6.006993000000	0.057586000000

H	-1.799891000000	-7.630697000000	0.052156000000
C	-0.423557000000	-6.095450000000	-0.591851000000
H	0.498835000000	-6.639769000000	-0.379451000000
H	-0.631006000000	-6.164294000000	-1.661928000000

**Table S5.** Gas phase geometries of the model  $\{\text{Cu}_4\text{I}_4(\text{L}^2)_4\}$  (the complex  $[\text{CuL}^2\text{I}]_n$ ) in Cartesian (XYZ) coordinates as calculated in Gaussian software at the B3LYP/LANL2DZ/D95V level of theory.

<b>Ground state (<math>S_0</math>)</b>			
I	3.360744000000	-0.777345000000	1.724092000000
Cu	2.825564000000	1.171609000000	-0.142422000000
S	4.344133000000	3.133966000000	-2.390379000000
C	4.202561000000	3.062339000000	1.584646000000
H	3.745873000000	2.384432000000	2.298982000000
N	4.005673000000	2.766456000000	0.269930000000
C	4.973966000000	4.164868000000	1.982143000000
H	5.125972000000	4.393620000000	3.030086000000
N	5.370102000000	4.652745000000	-0.349906000000
C	4.607074000000	3.578133000000	-0.656742000000
C	5.546511000000	4.944248000000	0.961624000000
H	6.160949000000	5.812807000000	1.181571000000
C	5.255923000000	4.264527000000	-4.782086000000
H	4.215970000000	4.344543000000	-5.120521000000
H	5.642410000000	3.283980000000	-5.085206000000
H	5.841214000000	5.033438000000	-5.302935000000
C	5.374869000000	4.476520000000	-3.267504000000
H	4.982120000000	5.444317000000	-2.949038000000
H	6.403195000000	4.381439000000	-2.911989000000
I	0.768562000000	0.777354000000	-1.724098000000
Cu	1.303732000000	-1.171599000000	0.142427000000
I	-0.768562000000	-0.777354000000	1.724098000000
Cu	-1.303732000000	1.171599000000	-0.142427000000
S	-1.141343000000	4.362563000000	-1.312660000000
C	-1.852546000000	2.819000000000	2.286059000000
H	-1.828480000000	1.811917000000	2.688866000000
N	-1.545036000000	2.940188000000	0.966129000000
C	-2.175470000000	3.929011000000	3.082215000000
H	-2.422490000000	3.813297000000	4.130828000000
N	-1.849943000000	5.328465000000	1.145314000000
C	-1.554662000000	4.208062000000	0.440676000000
C	-2.161108000000	5.186218000000	2.455243000000
H	-2.398739000000	6.099200000000	2.994594000000
C	-1.080187000000	6.560968000000	-3.037052000000
H	-1.799381000000	6.047604000000	-3.686460000000
H	-0.069129000000	6.270117000000	-3.347559000000
H	-1.187003000000	7.641498000000	-3.200293000000
C	-1.332529000000	6.241416000000	-1.557712000000
H	-2.342928000000	6.509493000000	-1.241747000000
H	-0.617628000000	6.735654000000	-0.895989000000
I	-3.360744000000	0.777345000000	-1.724092000000
Cu	-2.825564000000	-1.171609000000	0.142422000000
S	-4.344133000000	-3.133966000000	2.390379000000
C	-4.202561000000	-3.062339000000	-1.584646000000



H	-3.745873000000	-2.384432000000	-2.298982000000
N	-4.005673000000	-2.766456000000	-0.269930000000
C	-4.973966000000	-4.164868000000	-1.982143000000
H	-5.125972000000	-4.393620000000	-3.030086000000
N	-5.370102000000	-4.652745000000	0.349906000000
C	-4.607074000000	-3.578133000000	0.656742000000
C	-5.546511000000	-4.944248000000	-0.961624000000
H	-6.160949000000	-5.812807000000	-1.181571000000
C	-5.255923000000	-4.264527000000	4.782086000000
H	-4.215970000000	-4.344543000000	5.120521000000
H	-5.642410000000	-3.283980000000	5.085206000000
H	-5.841214000000	-5.033438000000	5.302935000000
C	-5.374869000000	-4.476520000000	3.267504000000
H	-4.982120000000	-5.444317000000	2.949038000000
H	-6.403195000000	-4.381439000000	2.911989000000
S	1.141343000000	-4.362563000000	1.312660000000
C	1.852546000000	-2.819000000000	-2.286059000000
H	1.828480000000	-1.811917000000	-2.688866000000
N	1.545036000000	-2.940188000000	-0.966129000000
C	2.175470000000	-3.929011000000	-3.082215000000
H	2.422490000000	-3.813297000000	-4.130828000000
N	1.849943000000	-5.328465000000	-1.145314000000
C	1.554662000000	-4.208062000000	-0.440676000000
C	2.161108000000	-5.186218000000	-2.455243000000
H	2.398739000000	-6.099200000000	-2.994594000000
C	1.080187000000	-6.560968000000	3.037052000000
H	1.799381000000	-6.047604000000	3.686460000000
H	0.069129000000	-6.270117000000	3.347559000000
H	1.187003000000	-7.641498000000	3.200293000000
C	1.332529000000	-6.241416000000	1.557712000000
H	2.342928000000	-6.509493000000	1.241747000000
H	0.617628000000	-6.735654000000	0.895989000000

**Lowest triplet excited state ( $T_1$ )**

I	3.360846000000	-0.777386000000	1.724025000000
Cu	2.825409000000	1.171670000000	-0.142291000000
S	4.730224000000	2.017481000000	-2.665773000000
C	4.244500000000	3.427047000000	1.048110000000
H	3.617410000000	3.134376000000	1.882413000000
N	4.108477000000	2.686199000000	-0.116378000000
C	5.157881000000	4.482706000000	1.130769000000
H	5.261997000000	5.052625000000	2.047738000000
N	5.814228000000	4.035417000000	-1.161595000000
C	4.922637000000	3.039695000000	-1.166235000000
C	5.939086000000	4.773781000000	-0.005087000000
H	6.669886000000	5.575094000000	-0.022225000000
C	6.018990000000	2.065357000000	-5.156071000000
H	5.040786000000	2.147728000000	-5.645104000000
H	6.260949000000	1.001232000000	-5.044103000000
H	6.768233000000	2.512528000000	-5.822444000000
C	6.039641000000	2.795809000000	-3.807688000000
H	5.789880000000	3.854480000000	-3.901491000000
H	7.002165000000	2.709665000000	-3.298840000000
I	0.768590000000	0.777198000000	-1.724116000000

Cu	1.303755000000	-1.171738000000	0.142445000000
I	-0.768590000000	-0.777198000000	1.724116000000
Cu	-1.303755000000	1.171738000000	-0.142445000000
S	0.090415000000	4.261403000000	0.194199000000
C	-3.048691000000	2.448864000000	1.858007000000
H	-3.483387000000	1.459536000000	1.766570000000
N	-1.935107000000	2.699829000000	1.103844000000
C	-3.604477000000	3.422202000000	2.696621000000
H	-4.488365000000	3.211554000000	3.286685000000
N	-1.861298000000	4.938988000000	1.989645000000
C	-1.383651000000	3.951000000000	1.204739000000
C	-2.969363000000	4.677641000000	2.733740000000
H	-3.334109000000	5.489799000000	3.355321000000
C	1.599754000000	6.573179000000	-0.268940000000
H	1.377982000000	6.483812000000	-1.339097000000
H	2.514573000000	6.006993000000	-0.057586000000
H	1.799891000000	7.630697000000	-0.052156000000
C	0.423557000000	6.095450000000	0.591851000000
H	-0.498835000000	6.639769000000	0.379451000000
H	0.631006000000	6.164294000000	1.661928000000
I	-3.360846000000	0.777386000000	-1.724025000000
Cu	-2.825409000000	-1.171670000000	0.142291000000
S	-4.730224000000	-2.017481000000	2.665773000000
C	-4.244500000000	-3.427047000000	-1.048110000000
H	-3.617410000000	-3.134376000000	-1.882413000000
N	-4.108477000000	-2.686199000000	0.116378000000
C	-5.157881000000	-4.482706000000	-1.130769000000
H	-5.261997000000	-5.052625000000	-2.047738000000
N	-5.814228000000	-4.035417000000	1.161595000000
C	-4.922637000000	-3.039695000000	1.166235000000
C	-5.939086000000	-4.773781000000	0.005087000000
H	-6.669886000000	-5.575094000000	0.022225000000
C	-6.018990000000	-2.065357000000	5.156071000000
H	-5.040786000000	-2.147728000000	5.645104000000
H	-6.260949000000	-1.001232000000	5.044103000000
H	-6.768233000000	-2.512528000000	5.822444000000
C	-6.039641000000	-2.795809000000	3.807688000000
H	-5.789880000000	-3.854480000000	3.901491000000
H	-7.002165000000	-2.709665000000	3.298840000000
S	-0.090415000000	-4.261403000000	-0.194199000000
C	3.048691000000	-2.448864000000	-1.858007000000
H	3.483387000000	-1.459536000000	-1.766570000000
N	1.935107000000	-2.699829000000	-1.103844000000
C	3.604477000000	-3.422202000000	-2.696621000000
H	4.488365000000	-3.211554000000	-3.286685000000
N	1.861298000000	-4.938988000000	-1.989645000000
C	1.383651000000	-3.951000000000	-1.204739000000
C	2.969363000000	-4.677641000000	-2.733740000000
H	3.334109000000	-5.489799000000	-3.355321000000
C	-1.599754000000	-6.573179000000	0.268940000000
H	-1.377982000000	-6.483812000000	1.339097000000
H	-2.514573000000	-6.006993000000	0.057586000000
H	-1.799891000000	-7.630697000000	0.052156000000
C	-0.423557000000	-6.095450000000	-0.591851000000

H	0.498835000000	-6.639769000000	-0.379451000000
H	-0.631006000000	-6.164294000000	-1.661928000000
<b>Lowest singlet excited state (S<sub>1</sub>)</b>			
I	3.360744000000	-0.777345000000	1.724092000000
Cu	2.825564000000	1.171609000000	-0.142422000000
S	4.200760000000	2.802664000000	-2.705976000000
C	4.312989000000	3.241639000000	1.280892000000
H	3.887087000000	2.687781000000	2.108621000000
N	4.007739000000	2.777088000000	0.002241000000
C	5.140955000000	4.350066000000	1.469256000000
H	5.374296000000	4.699447000000	2.469474000000
N	5.374283000000	4.529795000000	-0.940568000000
C	4.579170000000	3.462782000000	-1.042953000000
C	5.664253000000	4.993372000000	0.329875000000
H	6.311894000000	5.860699000000	0.390576000000
C	5.091419000000	3.527598000000	-5.262621000000
H	4.046822000000	3.612916000000	-5.586469000000
H	5.421050000000	2.495006000000	-5.431375000000
H	5.697738000000	4.184045000000	-5.900731000000
C	5.263422000000	3.942259000000	-3.795725000000
H	4.932763000000	4.965765000000	-3.608367000000
H	6.295626000000	3.845358000000	-3.452301000000
I	0.768562000000	0.777354000000	-1.724098000000
Cu	1.303732000000	-1.171599000000	0.142427000000
I	-0.768562000000	-0.777354000000	1.724098000000
Cu	-1.303732000000	1.171599000000	-0.142427000000
S	-1.046583000000	4.350584000000	-1.242216000000
C	-2.064447000000	2.780282000000	2.271107000000
H	-2.108489000000	1.769069000000	2.659975000000
N	-1.654656000000	2.913364000000	0.981337000000
C	-2.403838000000	3.888331000000	3.061144000000
H	-2.729778000000	3.767196000000	4.086896000000
N	-1.891002000000	5.303785000000	1.175989000000
C	-1.584508000000	4.186211000000	0.472640000000
C	-2.297240000000	5.153307000000	2.457524000000
H	-2.536668000000	6.066244000000	2.995623000000
C	-0.592928000000	6.571429000000	-2.875467000000
H	-1.247472000000	6.127944000000	-3.635354000000
H	0.429469000000	6.215197000000	-3.048842000000
H	-0.600502000000	7.659938000000	-3.016712000000
C	-1.071410000000	6.243981000000	-1.455442000000
H	-2.094619000000	6.577346000000	-1.270528000000
H	-0.419187000000	6.665021000000	-0.687603000000
I	-3.360744000000	0.777345000000	-1.724092000000
Cu	-2.825564000000	-1.171609000000	0.142422000000
S	-4.200760000000	-2.802664000000	2.705976000000
C	-4.312989000000	-3.241639000000	-1.280892000000
H	-3.887087000000	-2.687781000000	-2.108621000000
N	-4.007739000000	-2.777088000000	-0.002241000000
C	-5.140955000000	-4.350066000000	-1.469256000000
H	-5.374296000000	-4.699447000000	-2.469474000000
N	-5.374283000000	-4.529795000000	0.940568000000
C	-4.579170000000	-3.462782000000	1.042953000000
C	-5.664253000000	-4.993372000000	-0.329875000000

H	-6.311894000000	-5.860699000000	-0.390576000000
C	-5.091419000000	-3.527598000000	5.262621000000
H	-4.046822000000	-3.612916000000	5.586469000000
H	-5.421050000000	-2.495006000000	5.431375000000
H	-5.697738000000	-4.184045000000	5.900731000000
C	-5.263422000000	-3.942259000000	3.795725000000
H	-4.932763000000	-4.965765000000	3.608367000000
H	-6.295626000000	-3.845358000000	3.452301000000
S	1.046583000000	-4.350584000000	1.242216000000
C	2.064447000000	-2.780282000000	-2.271107000000
H	2.108489000000	-1.769069000000	-2.659975000000
N	1.654656000000	-2.913364000000	-0.981337000000
C	2.403838000000	-3.888331000000	-3.061144000000
H	2.729778000000	-3.767196000000	-4.086896000000
N	1.891002000000	-5.303785000000	-1.175989000000
C	1.584508000000	-4.186211000000	-0.472640000000
C	2.297240000000	-5.153307000000	-2.457524000000
H	2.536668000000	-6.066244000000	-2.995623000000
C	0.592928000000	-6.571429000000	2.875467000000
H	1.247472000000	-6.127944000000	3.635354000000
H	-0.429469000000	-6.215197000000	3.048842000000
H	0.600502000000	-7.659938000000	3.016712000000
C	1.071410000000	-6.243981000000	1.455442000000
H	2.094619000000	-6.577346000000	1.270528000000
H	0.419187000000	-6.665021000000	0.687603000000

Table S6. X-ray crystal structure and gas phase optimized geometries of the complex  $[\text{Cu}_2\text{L}^1\text{I}_2]_n$ . Hydrogen atoms are omitted for clarity. Plane  $\alpha$  is marked purple; plane  $\beta$  is marked orange.

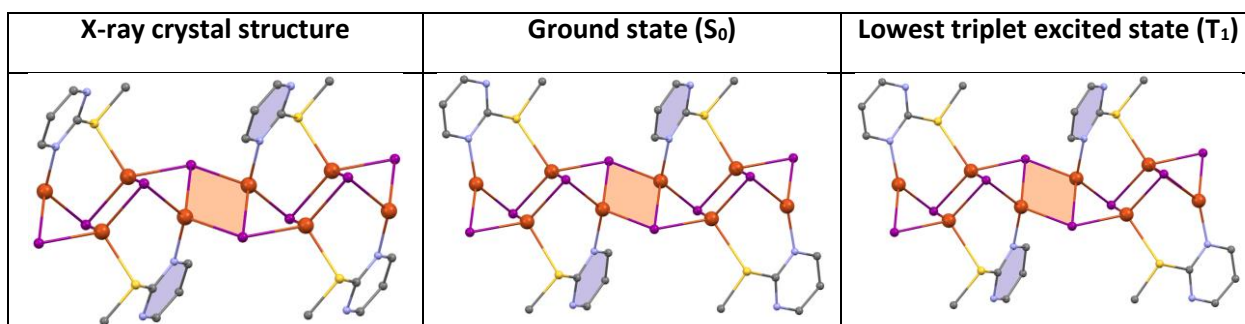
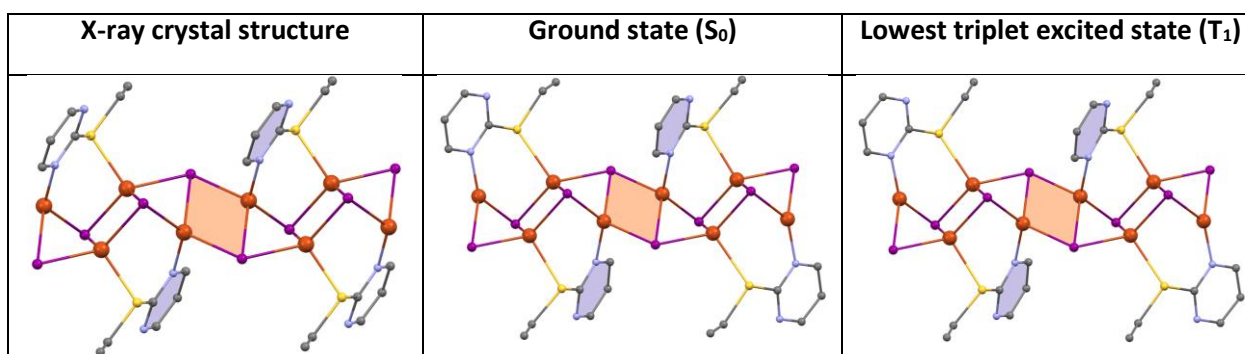


Table S7. X-ray crystal structure and gas phase optimized geometries of the complex  $[\text{Cu}_2\text{L}^2\text{I}_2]_n$ . Hydrogen atoms are omitted for clarity. Plane  $\alpha$  is marked purple; plane  $\beta$  is marked orange.



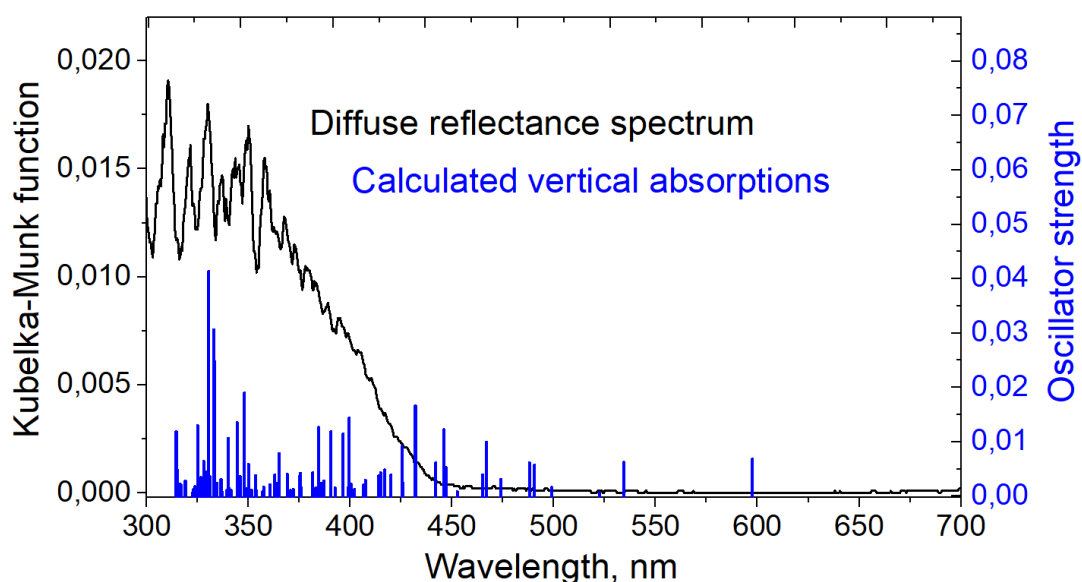


Figure S6. Diffuse reflectance spectrum of the complex  $[\text{Cu}_2\text{L}^1\text{I}_2]_n$  in the solid state (black). Vertical bars (blue) display the positions and oscillator strengths of the electronic transitions as calculated in Gaussian.

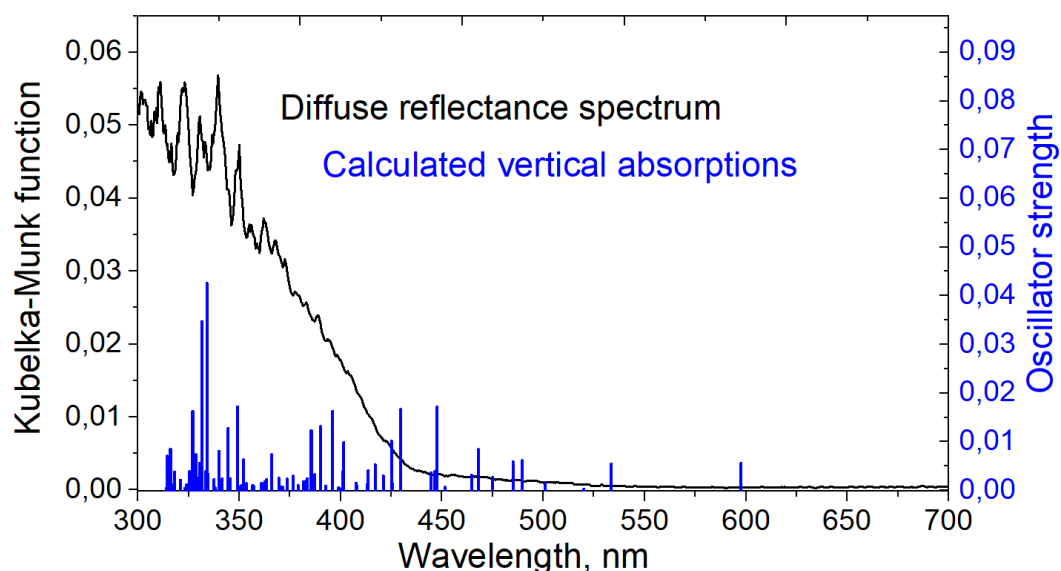


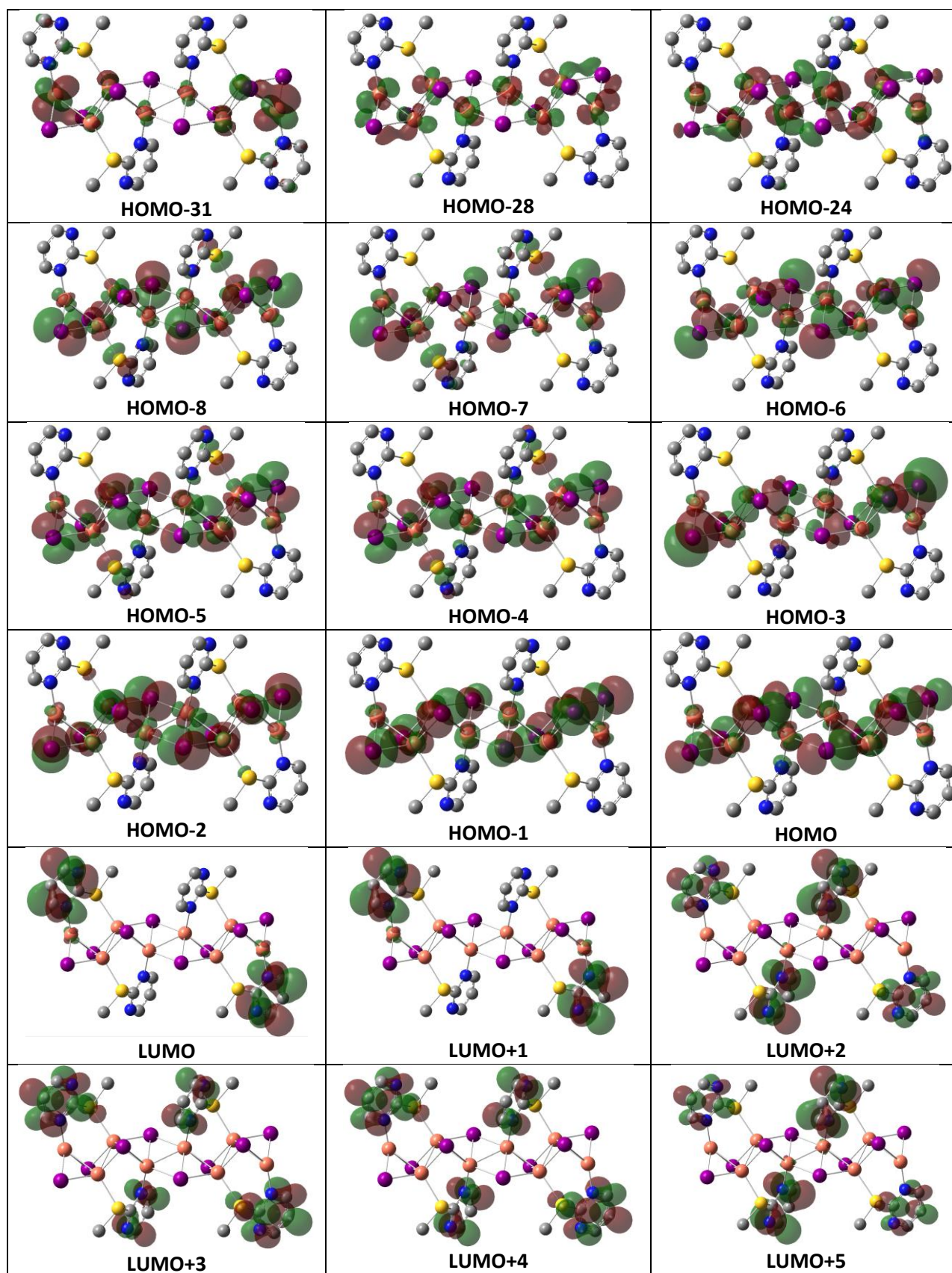
Figure S7. Diffuse reflectance spectrum of the complex  $[\text{Cu}_2\text{L}^2\text{I}_2]_n$  in the solid state (black). Vertical bars (blue) display the positions and oscillator strengths of the electronic transitions as calculated in Gaussian.

Table S8. Excited state properties of the model  $\{\text{Cu}_8\text{I}_8(\text{L}^1)_4\}$  (the complex  $[\text{Cu}_2\text{L}^1\text{I}_2]_n$ ) obtained from TD-DFT calculations in Gaussian software at the relaxed geometry of the ground state ( $S_0$ ). Transitions with contribution  $>10\%$  are shown.

State	Energy (eV)	Energy (nm)	Contributions (%)	Oscillator strength	Character
S1	2.0745	598	HOMO $\rightarrow$ LUMO+1 (67.9 %), HOMO-1 $\rightarrow$ LUMO (28.6 %)	0.0063	
S2	2.3194	535	HOMO-1 $\rightarrow$ LUMO (39.8 %), HOMO $\rightarrow$ LUMO+1 (25.6 %), HOMO-2 $\rightarrow$ LUMO+1 (21.0 %)	0.0057	
S3	2.3735	522	HOMO-3 $\rightarrow$ LUMO (35.7 %), HOMO-4 $\rightarrow$ LUMO+1 (21.3 %),	0.0001	

			HOMO-1 → LUMO (18.5 %), HOMO-2 → LUMO+1 (10.7 %)		XMLCT	
S4	2.4836	499	HOMO-5 → LUMO (36.1 %), HOMO-7 → LUMO+1 (25.7 %)	0.0011		
S5	2.5281	490	HOMO-2 → LUMO+1 (45.0 %), HOMO-4 → LUMO+1 (24.1 %), HOMO-10 → LUMO (10.2 %)	0.0051		
S6	2.5537	486	HOMO → LUMO+5 (56.2 %), HOMO → LUMO+3 (26.0 %)	0.0056		
S7	2.6148	474	HOMO-6 → LUMO+1 (30.9 %), HOMO-3 → LUMO (14.3 %), HOMO-10 → LUMO (13.5 %), HOMO-2 → LUMO+1 (12.6 %), HOMO-5 → LUMO (11.5 %)	0.0025		
S8	2.6538	467	HOMO-6 → LUMO+1 (25.6 %), HOMO-8 → LUMO (25.1 %), HOMO-9 → LUMO+1 (15.9 %)	0.0095		
S9	2.6659	465	HOMO → LUMO+3 (43.1 %), HOMO → LUMO+5 (22.5 %), HOMO-1 → LUMO+4 (15.3 %), HOMO-2 → LUMO+2 (11.1 %)	0.0034		
S10	2.7406	452	HOMO-4 → LUMO (37.1 %), HOMO-3 → LUMO+1 (23.8 %), HOMO-5 → LUMO+1 (17.0 %)	0.0003		
T1	2.0425	607	HOMO → LUMO+1 (62.2 %), HOMO-1 → LUMO (30.5 %)	0.0000		XMLCT
T2	2.3077	537	HOMO-1 → LUMO (34.5 %), HOMO → LUMO+1 (29.7 %), HOMO-2 → LUMO+1 (22.2 %)	0.0000		
T3	2.3606	525	HOMO-3 → LUMO (31.8 %), HOMO-4 → LUMO+1 (23.5 %), HOMO-1 → LUMO (12.6 %)	0.0000		
T4	2.4432	507	HOMO-7 → LUMO+1 (24.9 %), HOMO-5 → LUMO (23.3 %), HOMO-10 → LUMO (12.5 %), HOMO-1 → LUMO (11.6 %)	0.0000		
T5	2.4860	499	HOMO → LUMO+2 (55.4 %), HOMO → LUMO+4 (20.0 %)	0.0000		
T6	2.5002	496	HOMO → LUMO+5 (39.1 %), HOMO → LUMO+3 (18.2 %)	0.0000		
T7	2.5038	495	HOMO-2 → LUMO+1 (32.7 %), HOMO-4 → LUMO+1 (21.4 %)	0.0000		
T8	2.5939	478	HOMO-6 → LUMO+1 (30.0 %), HOMO-2 → LUMO+1 (12.4 %)	0.0000		
T9	2.6305	471	HOMO-8 → LUMO (26.7 %), HOMO-9 → LUMO+1 (20.4 %), HOMO-3 → LUMO (13.5 %), HOMO-5 → LUMO (12.7 %)	0.0000		
T10	2.6534	467	HOMO → LUMO+3 (45.6 %), HOMO → LUMO+5 (22.8 %), HOMO-1 → LUMO+4 (16.4 %), HOMO-1 → LUMO+2 (10.9 %)	0.0000		

Table S9. Iso-surface contour plots (iso-value = 0.02) of the model  $\{\text{Cu}_8\text{L}_8(\text{L}^1)_4\}$  (the complex  $[\text{Cu}_2\text{L}^1\text{L}_2]_n$ ) as calculated in Gaussian software at the ground state ( $S_0$ ) geometry.



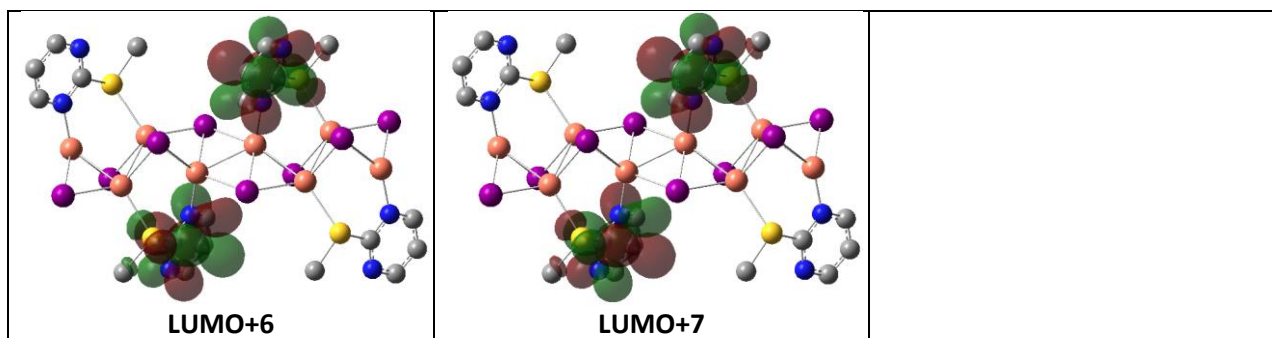


**Table S10.** Orbital energies and characters resulting from Mulliken population analysis calculated at the ground state ( $S_0$ ) optimized geometry of the model  $\{Cu_8I_8(L^1)_4\}$  (the complex  $[Cu_2L^1I_2]_n$ ).

Orbital	Energy (eV)	Contributions (%)		
		Cu	I	L
HOMO-31	-0.2646	87.5	8.4	4.1
HOMO-28	-0.2601	91.4	5.2	3.4
HOMO-24	-0.2539	86.0	10.5	3.5
HOMO-8	-0.2156	41.6	50.0	8.4
HOMO-7	-0.2137	41.2	47.3	11.5
HOMO-6	-0.2103	51.2	47.3	1.5
HOMO-5	-0.2090	46.8	44.0	9.2
HOMO-4	-0.2080	35.0	61.3	3.7
HOMO-3	-0.2053	30.6	67.0	2.4
HOMO-2	-0.2035	43.1	53.9	3.0
HOMO-1	-0.1965	41.8	56.5	1.7
HOMO	-0.1916	43.0	54.5	2.5
LUMO	-0.0978	2.8	0.5	96.8
LUMO+1	-0.0978	2.8	0.5	96.8
LUMO+2	-0.0766	2.7	0.3	97.0
LUMO+3	-0.0759	2.5	0.6	96.9
LUMO+4	-0.0753	2.1	0.7	97.2
LUMO+5	-0.0752	1.7	0.7	97.6
LUMO+6	-0.0565	2.4	0.5	97.1
LUMO+7	-0.0563	2.2	0.6	97.2

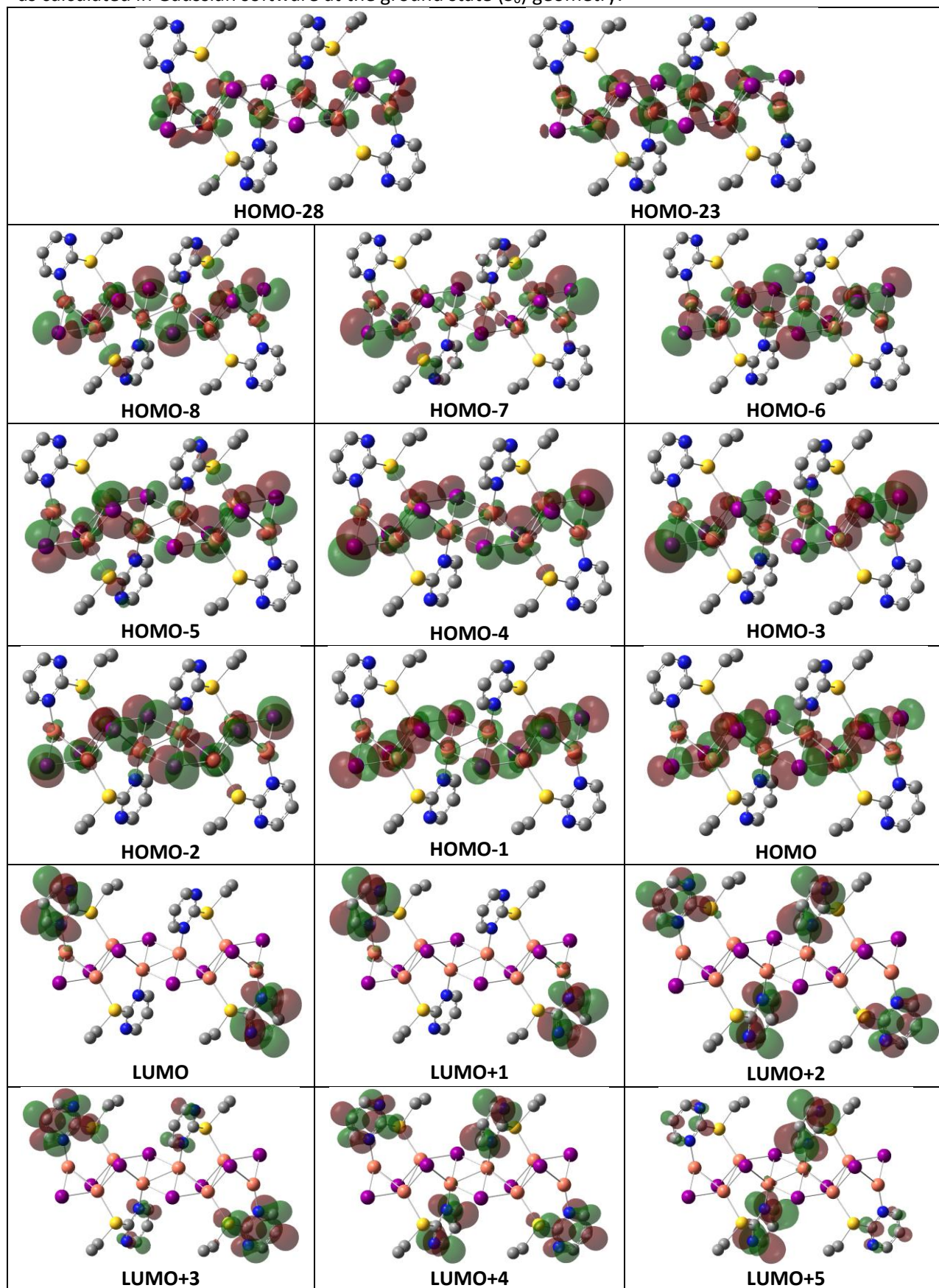
**Table S11.** Excited state properties of the model  $\{Cu_8I_8(L^2)_4\}$  (the complex  $[Cu_2L^2I_2]_n$ ) obtained from TD-DFT calculations in Gaussian software at the relaxed geometry of the ground state ( $S_0$ ). Transitions with contribution >10% are shown.

State	Energy (eV)	Energy (nm)	Contributions (%)	Oscillator strength	Character
S1	2.0754	597	HOMO $\rightarrow$ LUMO+1 (65.3 %), HOMO-1 $\rightarrow$ LUMO (30.7 %)	0.0055	
S2	2.3244	533	HOMO-1 $\rightarrow$ LUMO (44.3 %), HOMO $\rightarrow$ LUMO+1 (30.4 %), HOMO-2 $\rightarrow$ LUMO+1 (16.8 %)	0.0054	
S3	2.3832	520	HOMO-3 $\rightarrow$ LUMO (36.4 %), HOMO-4 $\rightarrow$ LUMO+1 (24.7 %), HOMO-2 $\rightarrow$ LUMO+1 (12.9 %), HOMO-1 $\rightarrow$ LUMO (12.2 %)	0.0002	



S4	2.4743	501	HOMO-5 → LUMO (37.9 %), HOMO-7 → LUMO+1 (21.8 %)	0.0014	XMLCT	
S5	2.5339	489	HOMO-2 → LUMO+1 (44.2 %), HOMO-4 → LUMO+1 (17.9 %), HOMO-10 → LUMO (13.1 %)	0.0061		
S6	2.5716	482	HOMO → LUMO+5 (67.3 %), HOMO → LUMO+3 (12.4 %)	0.0058		
S7	2.6094	475	HOMO-6 → LUMO+1 (35.7 %), HOMO-3 → LUMO (13.8 %), HOMO-10 → LUMO (13.7 %), HOMO-2 → LUMO+1 (12.8 %)	0.0026		
S8	2.6507	468	HOMO-8 → LUMO (25.6 %), HOMO-6 → LUMO+1 (20.9 %), HOMO-9 → LUMO+1 (15.4 %), HOMO-3 → LUMO (10.7 %)	0.0084		
S9	2.6679	465	HOMO-8 → LUMO (25.6 %), HOMO-6 → LUMO+1 (20.9 %), HOMO-9 → LUMO+1 (15.4 %), HOMO-3 → LUMO (10.7 %)	0.0031		
S10	2.7457	452	HOMO-4 → LUMO+1 (38.7 %), HOMO-5 → LUMO (21.1 %), HOMO-3 → LUMO (19.7 %)	0.0006		
T1	2.0450	606	HOMO → LUMO+1 (60.4 %), HOMO-1 → LUMO (32.1 %)	0.0000		XMLCT
T2	2.3130	536	HOMO-1 → LUMO (37.8 %), HOMO → LUMO+1 (33.9 %), HOMO-2 → LUMO+1 (18.8 %)	0.0000		
T3	2.3725	523	HOMO-3 → LUMO (31.5 %), HOMO-4 → LUMO+1 (27.9 %), HOMO-5 → LUMO (14.1 %), HOMO-2 → LUMO+1 (11.1 %)	0.0000		
T4	2.4385	508	HOMO-7 → LUMO+1 (22.7 %), HOMO-1 → LUMO (12.3 %), HOMO-3 → LUMO (12.1 %)	0.0000		
T5	2.5003	496	HOMO → LUMO+2 (39.5 %), HOMO → LUMO+4 (24.6 %)	0.0000		
T6	2.5043	495	HOMO-2 → LUMO+1 (37.1 %), HOMO-4 → LUMO+1 (20.0 %), HOMO-10 → LUMO (14.1 %)	0.0000		
T7	2.5152	493	HOMO → LUMO+5 (57.2 %), HOMO-1 → LUMO+2 (10.6 %)	0.0000		
T8	2.5869	479	HOMO-6 → LUMO+1 (31.0 %), HOMO-2 → LUMO+1 (12.1 %)	0.0000		
T9	2.6277	472	HOMO-8 → LUMO (24.0 %), HOMO-9 → LUMO+1 (18.3 %), HOMO-3 → LUMO (17.4 %), HOMO-2 → LUMO+1 (10.7 %), HOMO-5 → LUMO (10.3 %)	0.0000		
T10	2.6559	467	HOMO → LUMO+3 (55.0 %), HOMO-1 → LUMO+2 (15.1 %), HOMO-1 → LUMO+4 (13.7 %), HOMO → LUMO+5 (10.9 %)	0.0000		

Table S12. Iso-surface contour plots (iso-value = 0.02) of the model  $\{\text{Cu}_8\text{L}_8(\text{L}^2)_4\}$  (the complex  $[\text{Cu}_2\text{L}^2\text{I}_2]_n$ ) as calculated in Gaussian software at the ground state ( $S_0$ ) geometry.



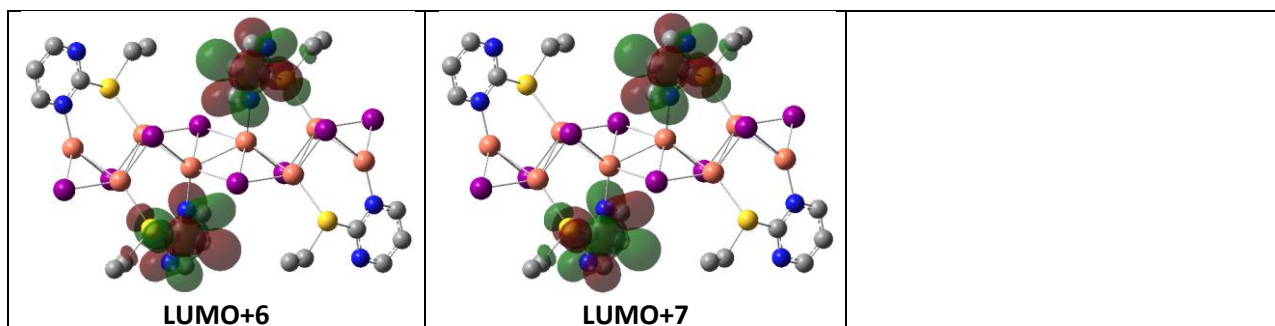


**Table S13.** Orbital energies and characters resulting from Mulliken population analysis calculated at the ground state ( $S_0$ ) optimized geometry of the model  $\{\text{Cu}_8\text{I}_8(\text{L}^2)_4\}$  (the complex  $[\text{Cu}_2\text{L}^2\text{I}_2]_n$ ).

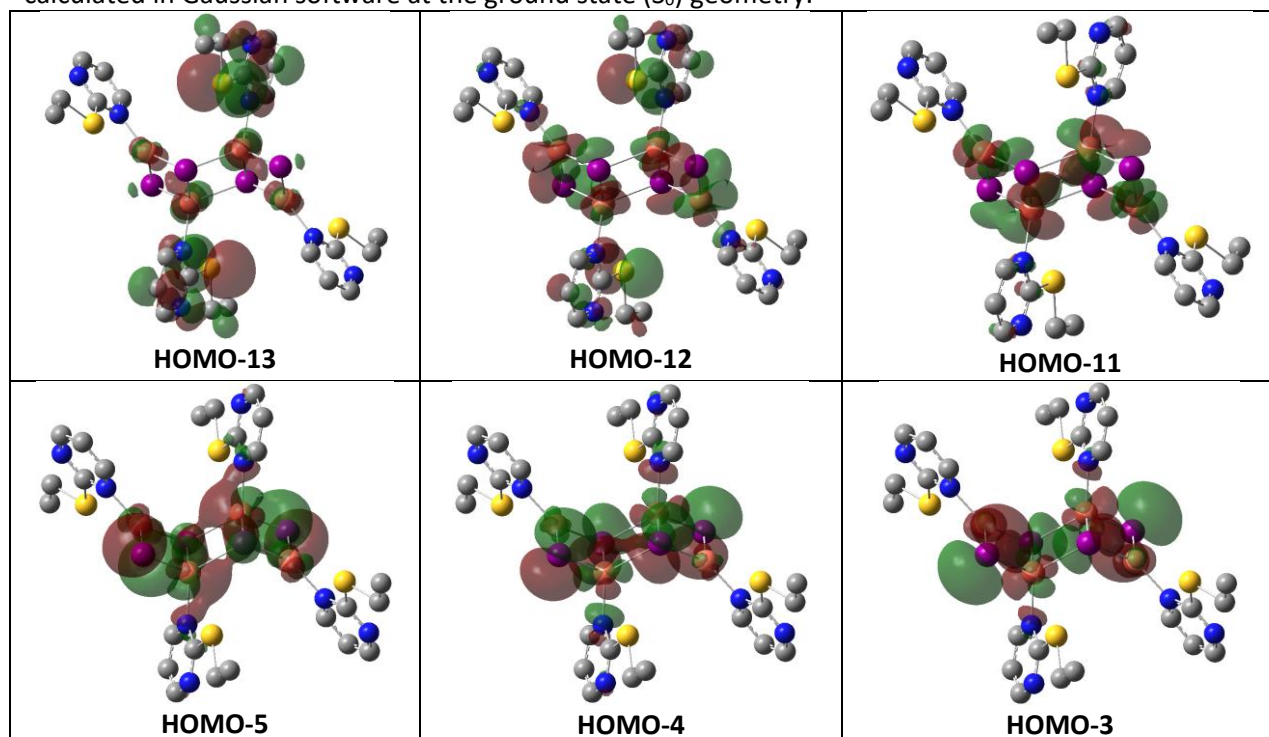
Orbital	Energy (eV)	Contributions (%)		
		Cu	I	L
HOMO-28	-0.2572	91.0	5.3	3.7
HOMO-23	-0.2513	87.1	9.6	3.3
HOMO-8	-0.2134	41.2	50.1	8.7
HOMO-7	-0.2114	41.8	45.7	12.5
HOMO-6	-0.2083	51.4	47.4	1.2
HOMO-5	-0.2064	46.0	45.3	8.7
HOMO-4	-0.2062	36.2	60.1	3.7
HOMO-3	-0.2035	32.5	64.5	3.0
HOMO-2	-0.2019	44.0	52.4	3.6
HOMO-1	-0.1943	41.9	56.3	1.8
HOMO	-0.1899	42.8	54.5	2.7
LUMO	-0.0957	2.8	0.5	96.7
LUMO+1	-0.0957	2.8	0.5	96.7
LUMO+2	-0.0744	2.8	0.3	96.9
LUMO+3	-0.0738	2.6	0.5	96.9
LUMO+4	-0.0731	2.1	0.7	97.2
LUMO+5	-0.0729	1.7	0.3	98.0
LUMO+6	-0.0544	2.3	0.5	97.2
LUMO+7	-0.0543	2.3	0.6	97.1

**Table S14.** Excited state properties of the model  $\{\text{Cu}_4\text{I}_4(\text{L}^2)_4\}$  (the complex  $[\text{CuL}^2\text{I}]_n$ ) obtained from TD-DFT calculations in Gaussian software at the relaxed geometry of the ground state ( $S_0$ ). Transitions with contribution >10% are shown.

State	Energy (eV)	Energy (nm)	Contributions (%)	Oscillator strength	Character
S1	1.9980	621	HOMO $\rightarrow$ LUMO (84.4 %), HOMO-2 $\rightarrow$ LUMO+1 (12.5 %)	0.0021	XMLCT
S2	2.2293	556	HOMO-1 $\rightarrow$ LUMO (56.0 %), HOMO-2 $\rightarrow$ LUMO+1 (27.1 %)	0.0161	
S3	2.3249	533	HOMO $\rightarrow$ LUMO+2 (87.8 %)	0.0158	
S4	2.3539	527	HOMO-2 $\rightarrow$ LUMO+1 (54.1 %), HOMO-1 $\rightarrow$ LUMO (36.3 %)	0.0081	
S5	2.4600	504	HOMO-3 $\rightarrow$ LUMO+1 (71.3 %), HOMO-4 $\rightarrow$ LUMO (22.0 %)	0.0060	
S6	2.5760	481	HOMO-1 $\rightarrow$ LUMO+2 (77.4 %)	0.0122	
S7	2.5807	480	HOMO-4 $\rightarrow$ LUMO (66.5 %), HOMO-3 $\rightarrow$ LUMO+1 (19.7 %)	0.0137	
S8	2.6480	468	HOMO $\rightarrow$ LUMO+5 (84.4 %)	0.0034	

S9	2.6576	467	HOMO-4 → LUMO+2 (38.2 %), HOMO-3 → LUMO+3 (19.8 %), HOMO-1 → LUMO+2 (12.4 %), HOMO-2 → LUMO+3 (12.2 %)	0.0041	XMLCT
S10	2.6864	462	HOMO-5 → LUMO+1 (86.2 %)	0.0039	
T1	1.9634	631	HOMO → LUMO (77.0 %), HOMO-2 → LUMO+1 (17.1 %)	0.0000	
T2	2.1776	569	HOMO-1 → LUMO (57.7 %), HOMO-2 → LUMO+1 (18.6 %), HOMO → LUMO (12.6 %)	0.0000	
T3	2.2390	554	HOMO → LUMO+2 (82.5 %)	0.0000	
T4	2.3346	531	HOMO-2 → LUMO+1 (54.0 %), HOMO-1 → LUMO (28.8 %)	0.0000	
T5	2.4429	508	HOMO-3 → LUMO+1 (64.9 %), HOMO-4 → LUMO (26.7 %)	0.0000	
T6	2.4922	498	HOMO-1 → LUMO+2 (57.3 %), HOMO-3 → LUMO+3 (17.0 %), HOMO-4 → LUMO+2 (11.6 %)	0.0000	
T7	2.5623	484	HOMO-4 → LUMO (52.9 %), HOMO-3 → LUMO+1 (26.2 %)	0.0000	
T8	2.5997	477	HOMO-4 → LUMO+2 (37.2 %), HOMO-1 → LUMO+2 (26.7 %), HOMO-5 → LUMO+3 (13.8 %), HOMO-3 → LUMO+3 (12.8 %)	0.0000	
T9	2.6381	470	HOMO → LUMO+5 (85.0 %)	0.0000	
T10	2.6751	463	HOMO-5 → LUMO+1 (75.1 %), HOMO-4 → LUMO (12.3 %)	0.0000	

Table S15. Iso-surface contour plots (iso-value = 0.02) of the model  $\{\text{Cu}_4\text{I}_4(\text{L}^2)_4\}$  (the complex  $[\text{CuL}^2\text{I}]_n$ ) as calculated in Gaussian software at the ground state ( $S_0$ ) geometry.



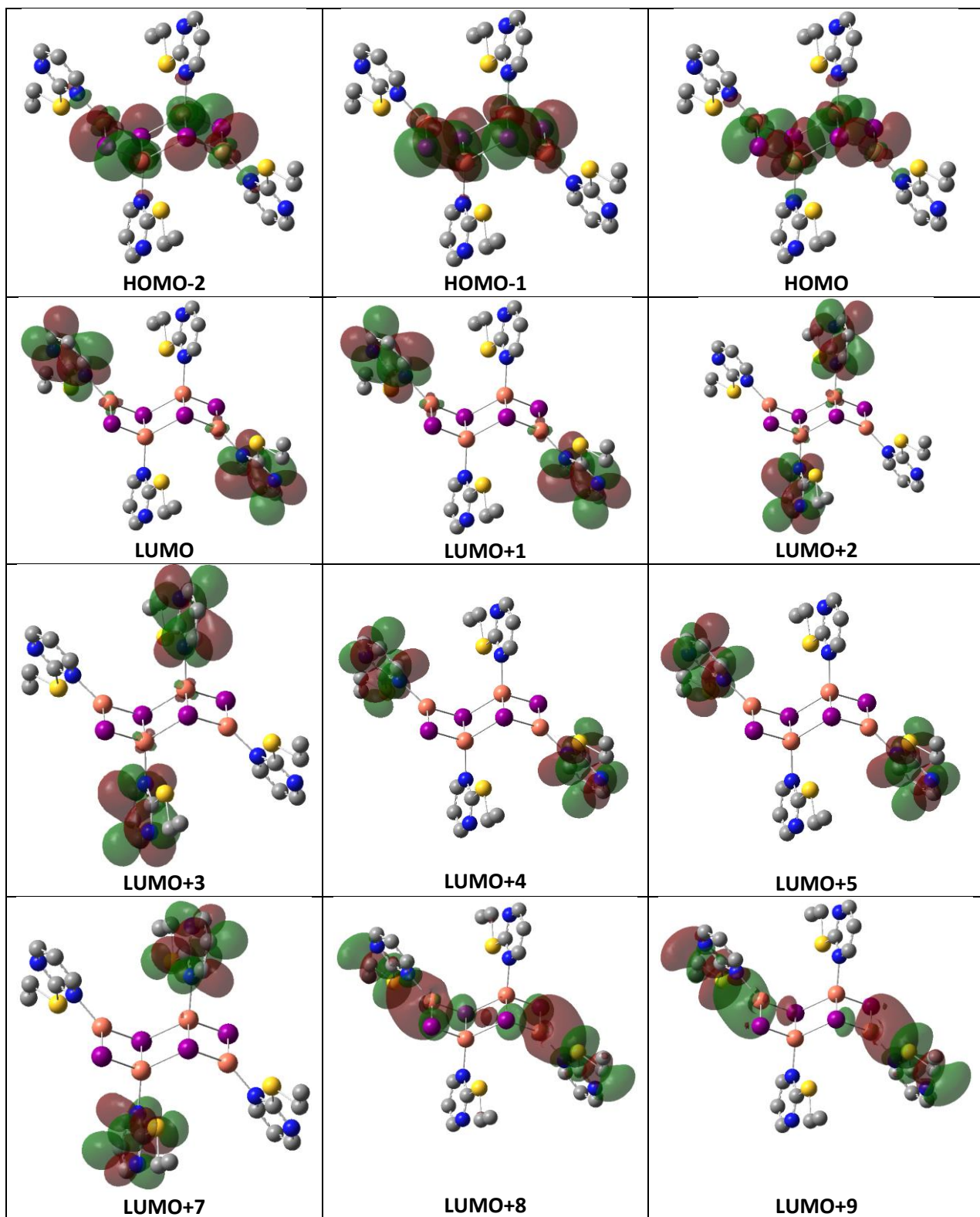


**Table S16.** Orbital energies and characters resulting from Mulliken population analysis calculated at the ground state ( $S_0$ ) optimized geometry of the model  $\{Cu_4I_4(L^2)_4\}$  (the complex  $[CuL^2I]_n$ ).

Orbital	Energy (eV)	Contributions (%)		
		Cu	I	L
HOMO-13	-0.2293	21.7	3.0	75.3
HOMO-12	-0.2270	53.9	12.8	33.3
HOMO-11	-0.2246	82.1	12.6	5.3
HOMO-5	-0.1921	57.6	36.6	5.8
HOMO-4	-0.1879	49.8	44.0	6.2
HOMO-3	-0.1860	37.7	59.1	3.2
HOMO-2	-0.1802	45.0	50.4	4.6
HOMO-1	-0.1786	48.5	49.6	1.9
HOMO	-0.1697	45.5	50.8	3.7
LUMO	-0.0768	2.1	0.3	97.6
LUMO+1	-0.0767	2.0	0.4	97.6
LUMO+2	-0.0618	1.6	0.5	97.9
LUMO+3	-0.0618	1.6	0.5	97.9
LUMO+4	-0.0538	1.2	0.2	98.6
LUMO+5	-0.0539	1.1	0.2	98.7
LUMO+7	-0.0404	1.1	0.2	98.7
LUMO+8	0.0022	45.6	4.8	49.6
LUMO+9	0.0058	29.1	2.5	68.4

**Table S17.** Excited state properties of the model  $\{Cu_8I_8(L^1)_4\}$  (the complex  $[Cu_2L^1I_2]_n$ ) obtained from TD-DFT calculations in Gaussian software at the relaxed geometry of the lowest triplet excited state ( $T_1$ ). Transitions with contribution >10% are shown.

State	Energy (eV)	Energy (nm)	Contributions (%)	Oscillator strength	Character
S1	1.8052	687	HOMO $\rightarrow$ LUMO (72.5 %), HOMO-1 $\rightarrow$ LUMO+1 (24.9 %)	0.0071	XMLCT
S2	2.0368	609	HOMO-1 $\rightarrow$ LUMO+1 (46.2 %), HOMO $\rightarrow$ LUMO (22.9 %), HOMO-2 $\rightarrow$ LUMO (20.6 %)	0.0071	
S3	2.0965	591	HOMO-3 $\rightarrow$ LUMO+1 (37.2 %), HOMO-4 $\rightarrow$ LUMO (26.1 %), HOMO-1 $\rightarrow$ LUMO+1 (15.8 %)	0.0001	
T1	1.7688	701	HOMO $\rightarrow$ LUMO (65.4 %), HOMO-1 $\rightarrow$ LUMO+1 (27.9 %)	0.0000	XMLCT
T2	2.0211	613	HOMO-1 $\rightarrow$ LUMO+1 (38.4 %), HOMO $\rightarrow$ LUMO (28.2 %), HOMO-2 $\rightarrow$ LUMO (22.5 %)	0.0000	
T3	2.0814	596	HOMO-3 $\rightarrow$ LUMO+1 (33.1 %), HOMO-4 $\rightarrow$ LUMO (29.0 %), HOMO-1 $\rightarrow$ LUMO+1 (11.4 %)	0.0000	

**Table S18.** Iso-surface contour plots (iso-value = 0.02) of the model  $\{\text{Cu}_8\text{l}_8(\text{L}^1)_4\}$  (the complex  $[\text{Cu}_2\text{L}^1\text{I}_2]_n$ ) as calculated in Gaussian software at the lowest triplet excited state ( $T_1$ ) geometry.

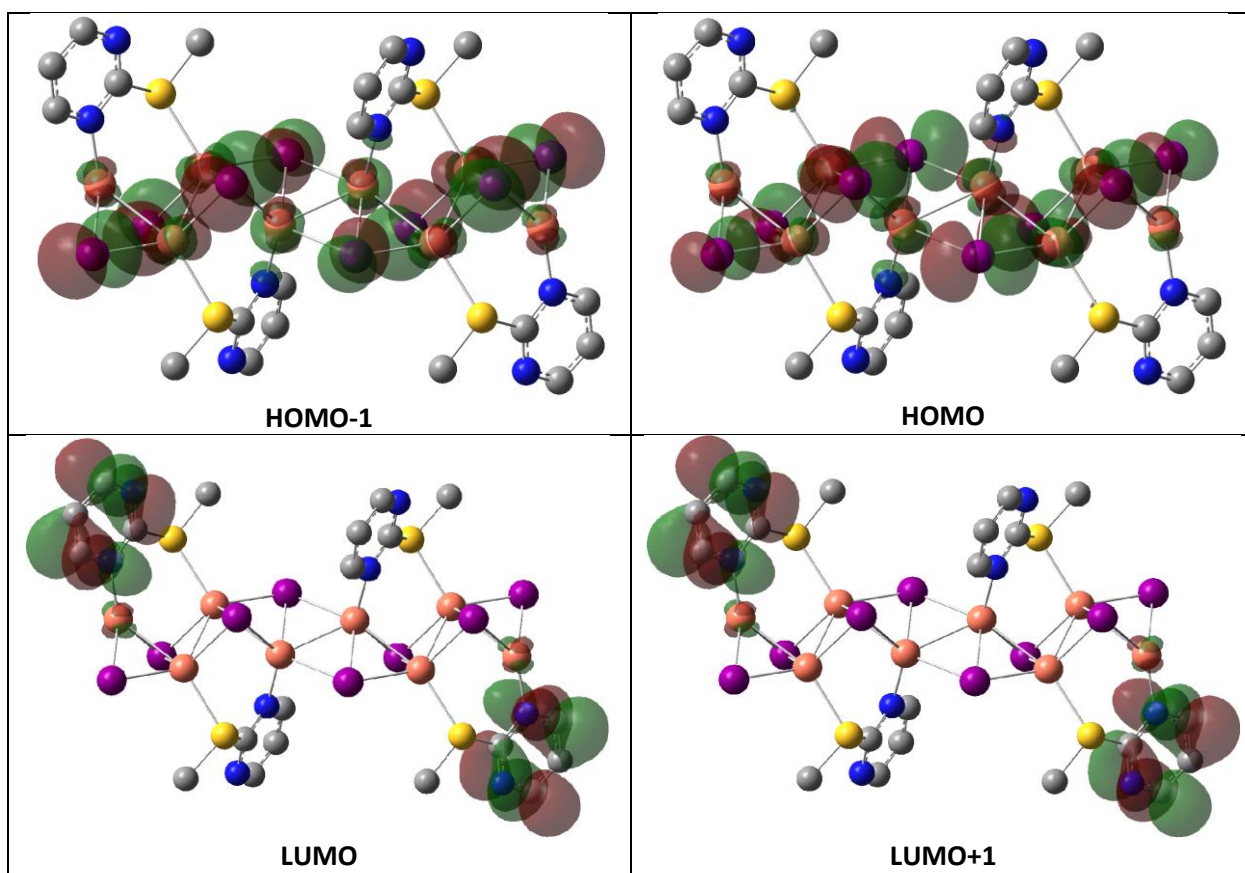


**Table S19.** Orbital energies and characters resulting from Mulliken population analysis calculated at the lowest triplet excited state ( $T_1$ ) optimized geometry of the model  $\{\text{Cu}_8\text{l}_8(\text{L}^1)_4\}$  (the complex  $[\text{Cu}_2\text{L}^1\text{I}_2]_n$ ).

Orbital	Energy (eV)	Contributions (%)		
		Cu	I	L
HOMO-1	-0.1951	41.7	56.5	1.8
HOMO	-0.1898	43.2	53.9	2.9
LUMO	-0.1067	2.9	0.5	96.6
LUMO+1	-0.1067	2.9	0.6	96.5

**Table S20.** Excited state properties of the model  $\{\text{Cu}_8\text{l}_8(\text{L}^2)_4\}$  (the complex  $[\text{Cu}_2\text{L}^2\text{I}_2]_n$ ) obtained from TD-DFT calculations in Gaussian software at the relaxed geometry of the lowest triplet excited state ( $T_1$ ). Transitions with contribution >10% are shown.

State	Energy (eV)	Energy (nm)	Contributions (%)	Oscillator strength	Character
S1	1.7821	696	HOMO $\rightarrow$ LUMO (68.6 %), HOMO-1 $\rightarrow$ LUMO+1 (28.2 %)	0.0066	XMLCT
S2	2.0196	614	HOMO-1 $\rightarrow$ LUMO+1 (49.5 %), HOMO $\rightarrow$ LUMO (28.1 %), HOMO-2 $\rightarrow$ LUMO (16.2 %)	0.0067	
S3	2.0829	595	HOMO-3 $\rightarrow$ LUMO+1 (36.3 %), HOMO-4 $\rightarrow$ LUMO (30.1 %), HOMO-5 $\rightarrow$ LUMO+1 (10.9 %)	0.0004	

T1	1.7457	710	HOMO → LUMO (62.1 %), HOMO-1 → LUMO+1 (30.5 %)	0.0000	XMLCT
T2	2.0048	618	HOMO-1 → LUMO+1 (40.2 %), HOMO → LUMO (32.4 %), HOMO-2 → LUMO (19.3 %)	0.0000	
T3	2.0709	599	HOMO-4 → LUMO (32.9 %), HOMO-3 → LUMO+1 (31.4 %), HOMO-5 → LUMO+1 (15.6 %)	0.0000	

Table S21. Iso-surface contour plots (iso-value = 0.02) of the model  $\{\text{Cu}_8\text{l}_8(\text{L}^2)_4\}$  (the complex  $[\text{Cu}_2\text{L}^2\text{I}_2]_n$ ) as calculated in Gaussian software at the lowest triplet excited state ( $T_1$ ) geometry.

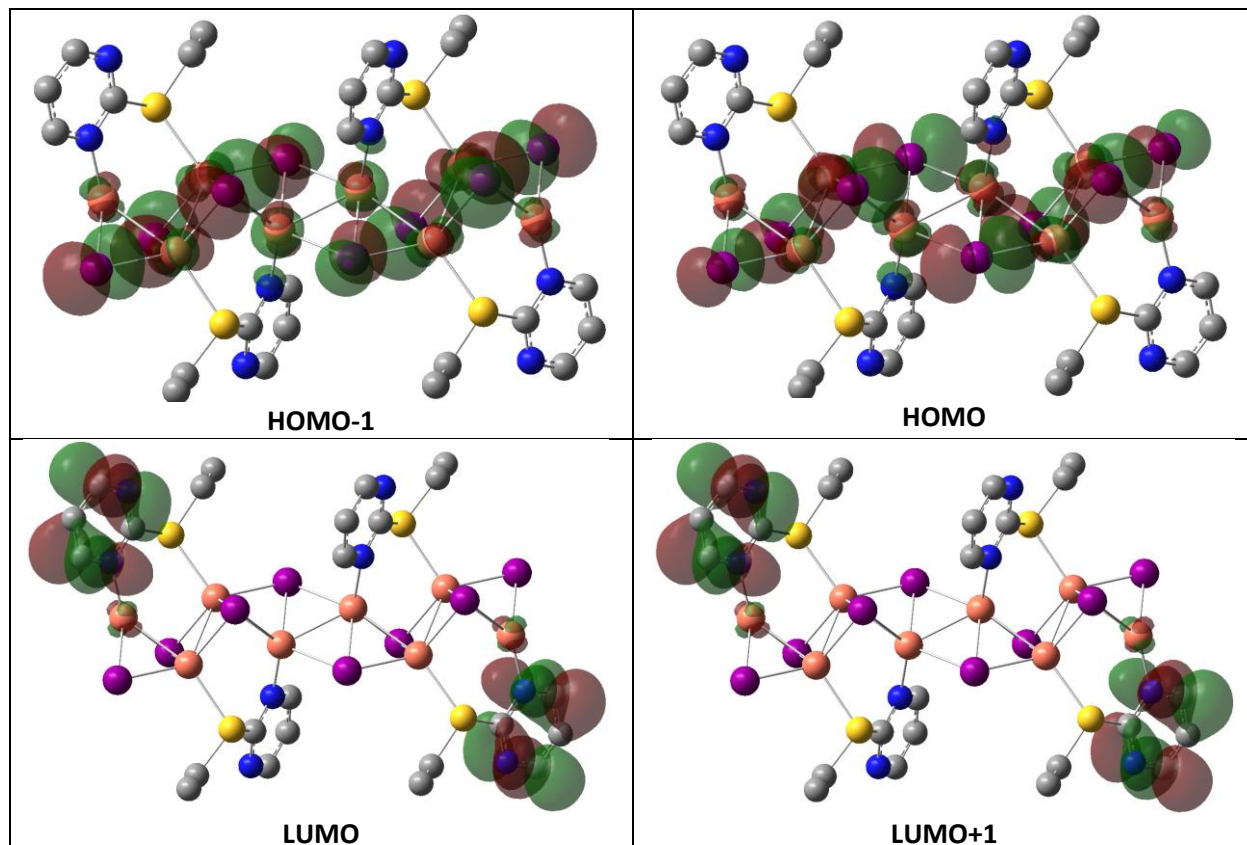


Table S22. Orbital energies and characters resulting from Mulliken population analysis calculated at the lowest triplet excited state ( $T_1$ ) optimized geometry of the model  $\{\text{Cu}_8\text{l}_8(\text{L}^2)_4\}$  (the complex  $[\text{Cu}_2\text{L}^2\text{I}_2]_n$ ).

Orbital	Energy (eV)	Contributions (%)		
		Cu	I	L
HOMO-1	-0.1930	41.7	56.2	2.1
HOMO	-0.1884	42.9	54.1	3.0
LUMO	-0.1056	2.9	0.5	96.6
LUMO+1	-0.0739	2.9	0.6	96.5



**Table S23.** Excited state properties of the model  $\{\text{Cu}_4\text{I}_4(\text{L}^2)_4\}$  (the complex  $[\text{CuL}^2\text{I}]_n$ ) obtained from TD-DFT calculations in Gaussian software at the relaxed geometry of the lowest triplet excited state ( $T_1$ ). Transitions with contribution >10% are shown.

State	Energy (eV)	Energy (nm)	Contributions (%)	Oscillator strength	Character
S1	1.5867	781	HOMO $\rightarrow$ LUMO (93.2 %)	0.0027	XMLCT
S2	1.9702	629	HOMO-2 $\rightarrow$ LUMO+1 (57.8 %), HOMO-1 $\rightarrow$ LUMO (30.7 %)	0.0227	
S3	2.0117	616	HOMO-1 $\rightarrow$ LUMO (64.9 %), HOMO-2 $\rightarrow$ LUMO+1 (30.9 %)	0.0159	
T1	1.5593	795	HOMO $\rightarrow$ LUMO (90.0 %)	0.0000	XMLCT
T2	1.8684	664	HOMO-1 $\rightarrow$ LUMO (66.0 %), HOMO-2 $\rightarrow$ LUMO+1 (14.8 %)	0.0000	
T3	1.9780	627	HOMO-2 $\rightarrow$ LUMO+1 (57.3 %), HOMO-1 $\rightarrow$ LUMO (16.6 %), HOMO $\rightarrow$ LUMO+3 (12.2 %)	0.0000	

**Table S24.** Iso-surface contour plots (iso-value = 0.02) of the model  $\{\text{Cu}_4\text{I}_4(\text{L}^2)_4\}$  (the complex  $[\text{CuL}^2\text{I}]_n$ ) as calculated in Gaussian software at the lowest triplet excited state ( $T_1$ ) geometry.

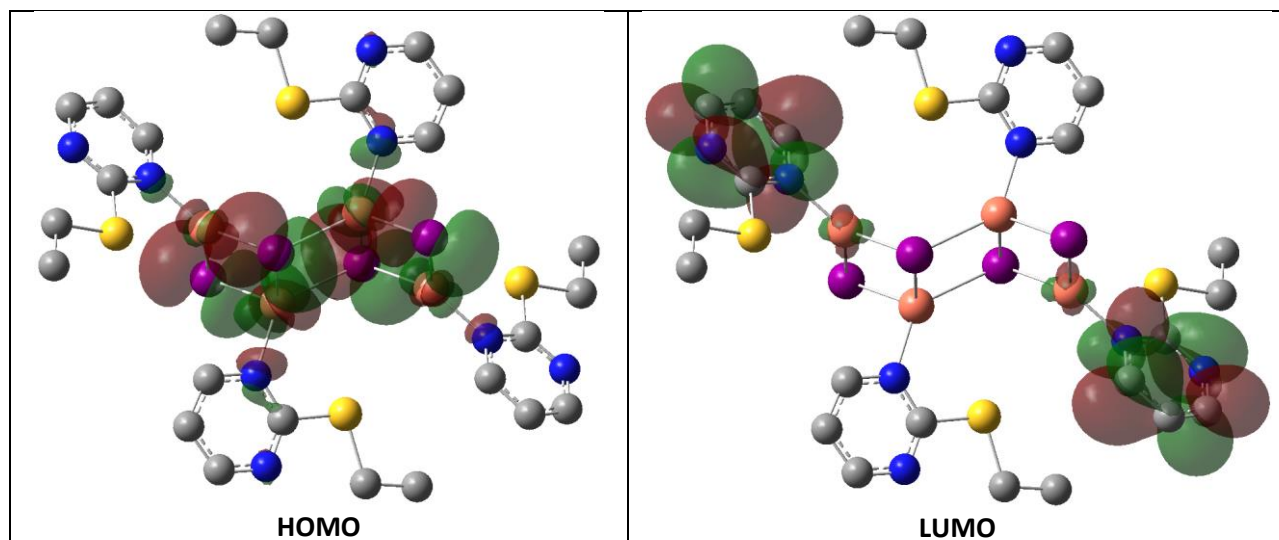
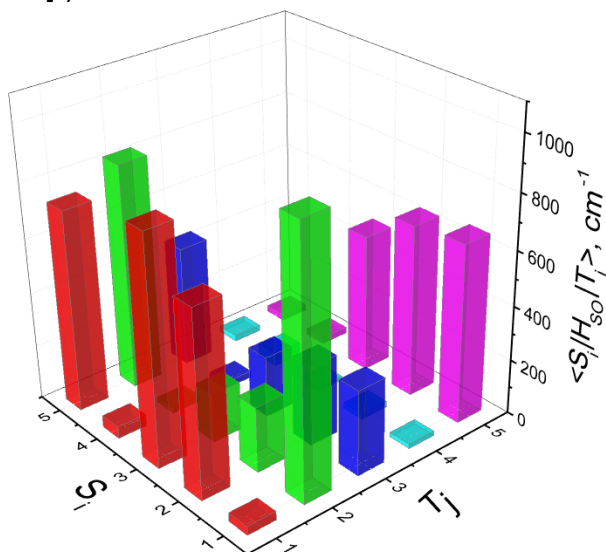


**Table S25.** Orbital energies and characters resulting from Mulliken population analysis calculated at the lowest triplet excited state ( $T_1$ ) optimized geometry of the model  $\{\text{Cu}_4\text{I}_4(\text{L}^2)_4\}$  (the complex  $[\text{CuL}^2\text{I}]_n$ ).

Orbital	Energy (eV)	Contributions (%)		
		Cu	I	L
HOMO	-0.1635	45.4	49.9	4.7
LUMO	-0.0867	2.3	0.8	96.9

Table S26. Spin-orbit couplings  $\langle S_i | H_{so} | T_j \rangle$  calculated as root mean squares in ADF for the model  $\{Cu_4I_4(L^2)_4\}$  (the complex  $[CuL^2I]_n$ ).



$\langle S_i   H_{so}   T_j \rangle, \text{cm}^{-1}$	T1	T2	T3	T4	T5
S1	32,13	966,05	313,28	16,69	653,16
S2	678,9	240,35	292,17	21,4	632,32
S3	837,18	178,21	223,65	15,26	507,9
S4	43,5	19	24,52	47,74	23,23
S5	738,09	826,23	445,51	21,95	22,38

Table S27. Excited state properties of the model  $\{Cu_4I_4(L^2)_4\}$  (the complex  $[CuL^2I]_n$ ) obtained from TD-DFT calculations in Gaussian software at the relaxed geometry of the lowest singlet excited state ( $S_1$ ). Transitions with contribution  $>10\%$  are shown.

State	Energy (eV)	Energy (nm)	Contributions (%)	Oscillator strength	Character
S1	1.6607	747	HOMO $\rightarrow$ LUMO (90.2 %)	0.0022	XMLCT
S2	1.9673	630	HOMO-2 $\rightarrow$ LUMO+1 (33.4 %), HOMO-1 $\rightarrow$ LUMO (54.0 %)	0.0176	
S3	2.0547	603	HOMO-1 $\rightarrow$ LUMO (40.6 %), HOMO-2 $\rightarrow$ LUMO+1 (51.6 %)	0.0085	
T1	1.6296	761	HOMO $\rightarrow$ LUMO (85.4 %)	0.0000	XMLCT
T2	1.8973	653	HOMO-1 $\rightarrow$ LUMO (62.1 %), HOMO-2 $\rightarrow$ LUMO+1 (19.6 %)	0.0000	
T3	2.0281	611	HOMO-2 $\rightarrow$ LUMO+1 (57.8 %), HOMO-1 $\rightarrow$ LUMO (24.4 %)	0.0000	

**Table S28.** Iso-surface contour plots (iso-value = 0.02) of the model  $\{\text{Cu}_4\text{I}_4(\text{L}^2)_4\}$  (the complex  $[\text{CuL}^2\text{I}]_n$ ) as calculated in Gaussian software at the lowest singlet excited state ( $S_1$ ) geometry.

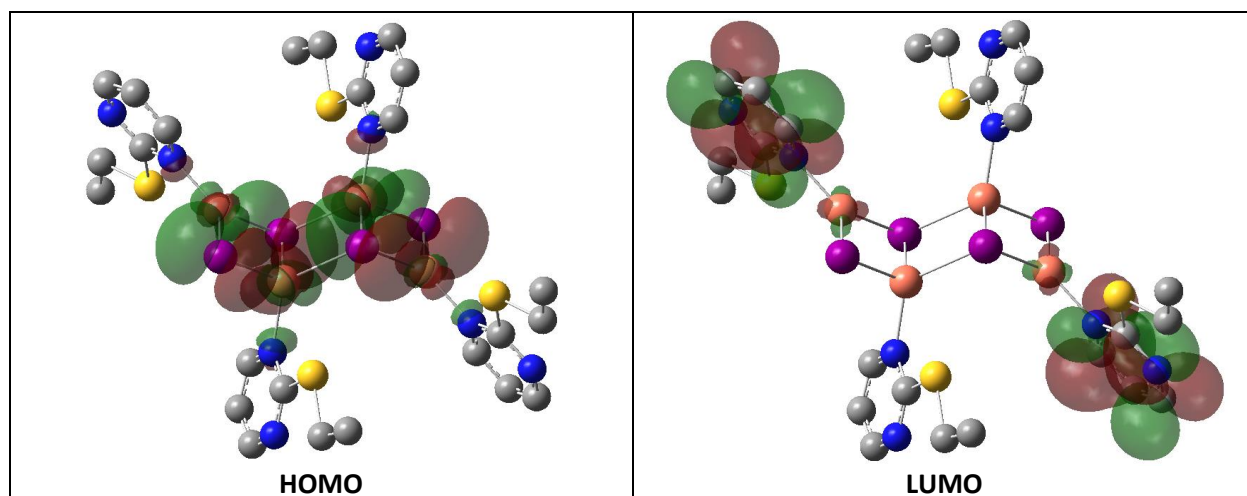


**Table S29.** Orbital energies and characters resulting from Mulliken population analysis calculated at the lowest singlet excited state ( $S_1$ ) optimized geometry of the model  $\{\text{Cu}_4\text{I}_4(\text{L}^2)_4\}$  (the complex  $[\text{CuL}^2\text{I}]_n$ ).

Orbital	Energy (eV)	Contributions (%)		
		Cu	I	L
HOMO	-0.1662	45.2	50.7	4.1
LUMO	-0.0862	2.4	0.5	97.1

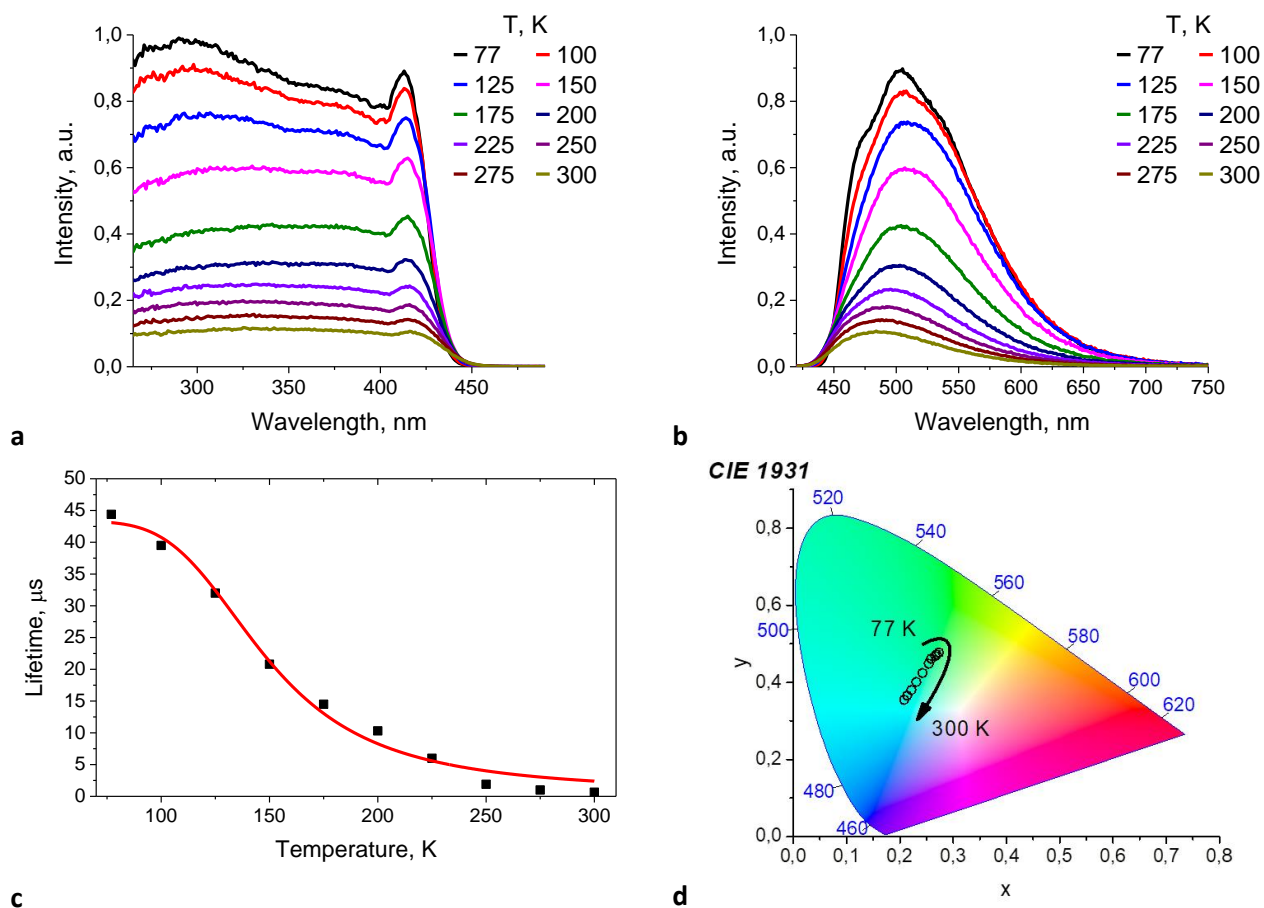


Figure S8. Luminescence properties of the complex  $[\text{Cu}_2\text{L}^2\text{I}_2]_n$ . Temperature dependence a) of the excitation spectra,  $\lambda_{\text{em}} = 500 \text{ nm}$ ; b) of the luminescence spectra,  $\lambda_{\text{ex}} = 410 \text{ nm}$ ; c) of the photoluminescence decay time; d) of the photoluminescence chromaticity,  $\lambda_{\text{ex}} = 410 \text{ nm}$ .

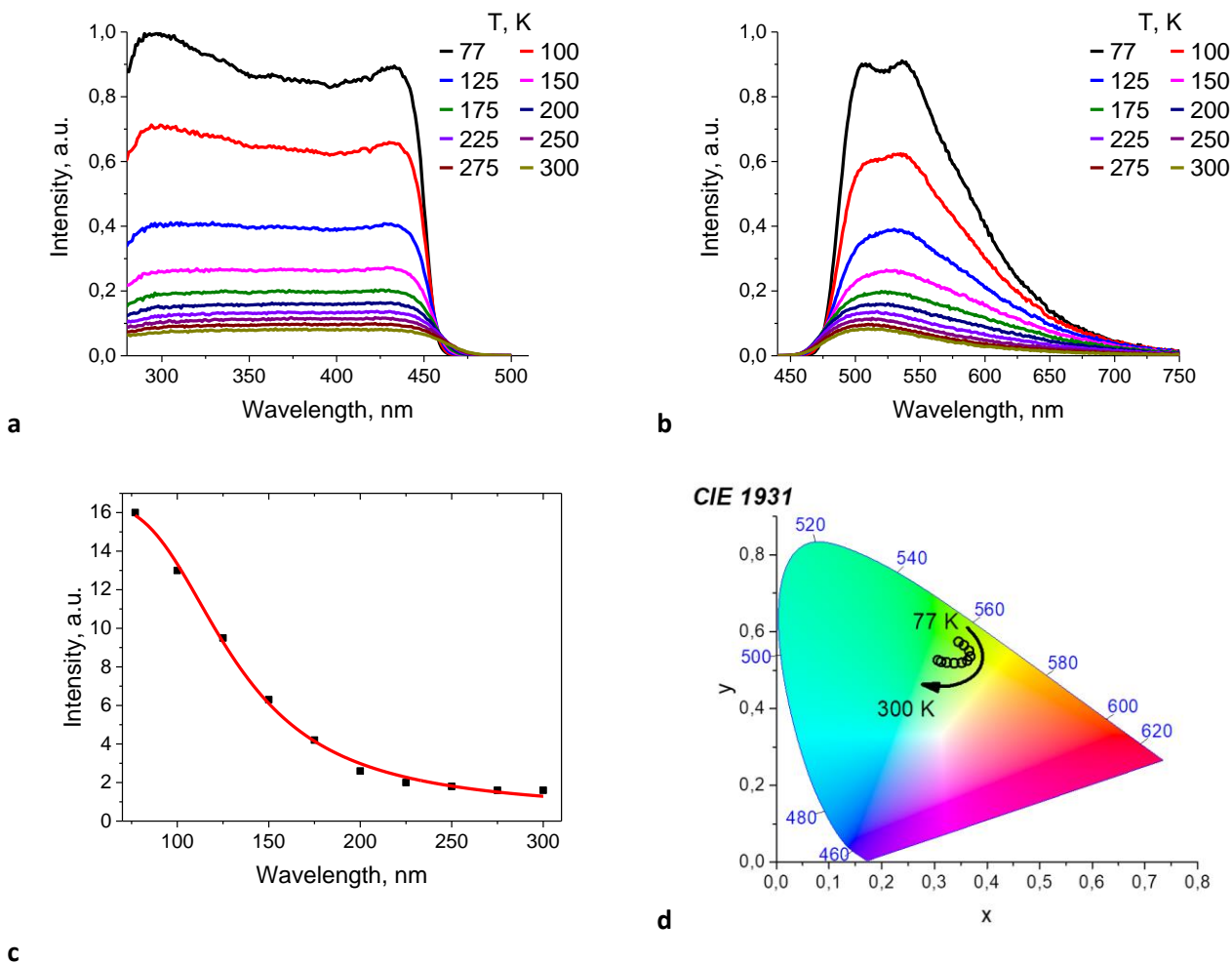
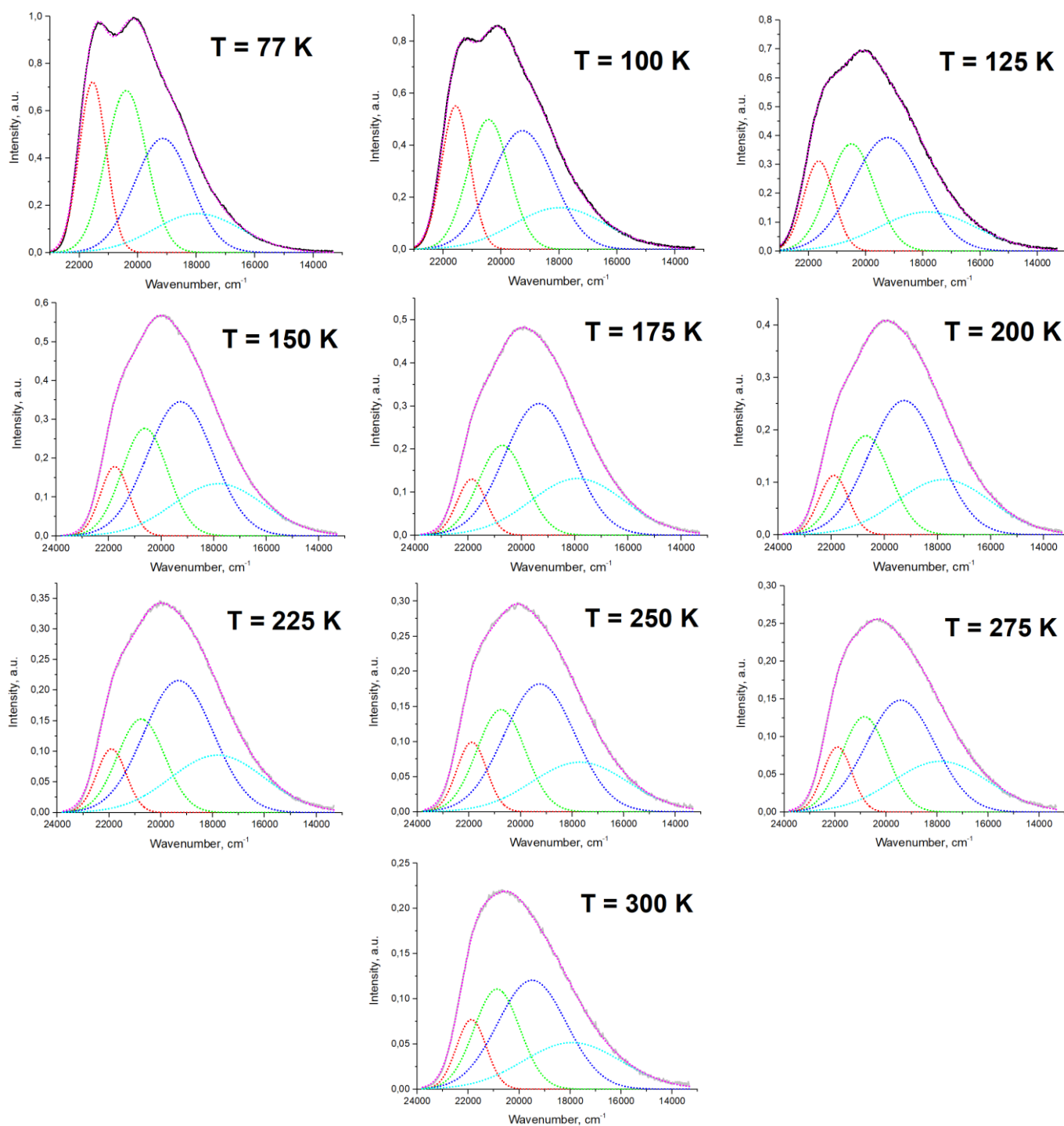


Figure S9. Luminescence properties of the complex  $[\text{CuL}^2\text{I}]_n$ . Temperature dependence a) of the excitation spectra,  $\lambda_{\text{em}} = 510$  nm; b) of the luminescence spectra,  $\lambda_{\text{ex}} = 430$  nm; c) of the photoluminescence decay time; d) of the photoluminescence chromaticity,  $\lambda_{\text{ex}} = 410$  nm.

Table S30. The emission spectra of the complex  $[\text{Cu}_2\text{L}^1\text{I}_2]_n$  at  $T = 77\text{--}300\text{ K}$  resolved into four Gauss functions.



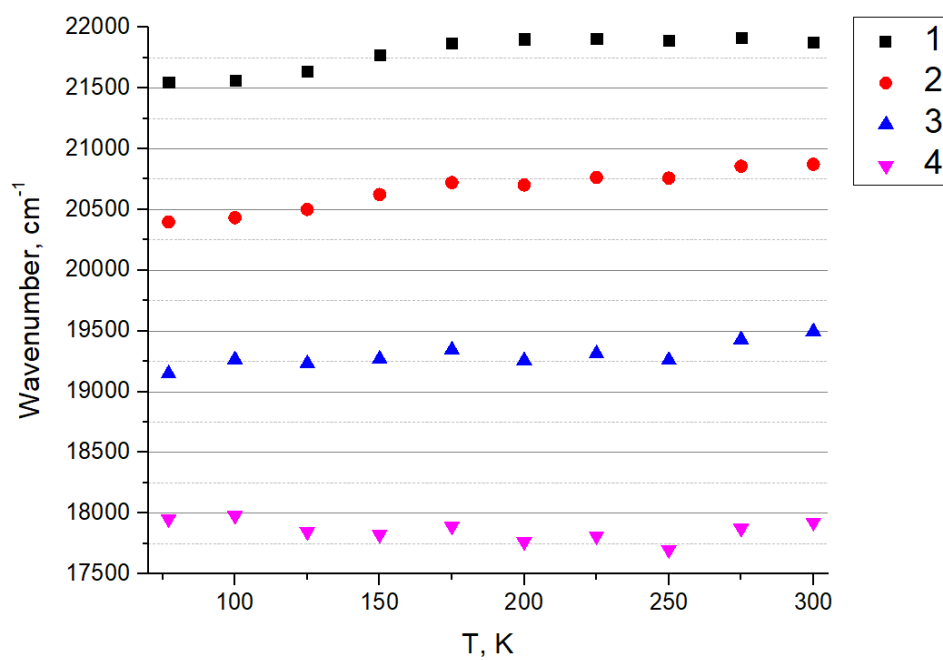


Figure S10. Temperature dependence of the maxima of the Gauss functions for the complex  $[\text{Cu}_2\text{L}^1\text{I}_2]_n$ .

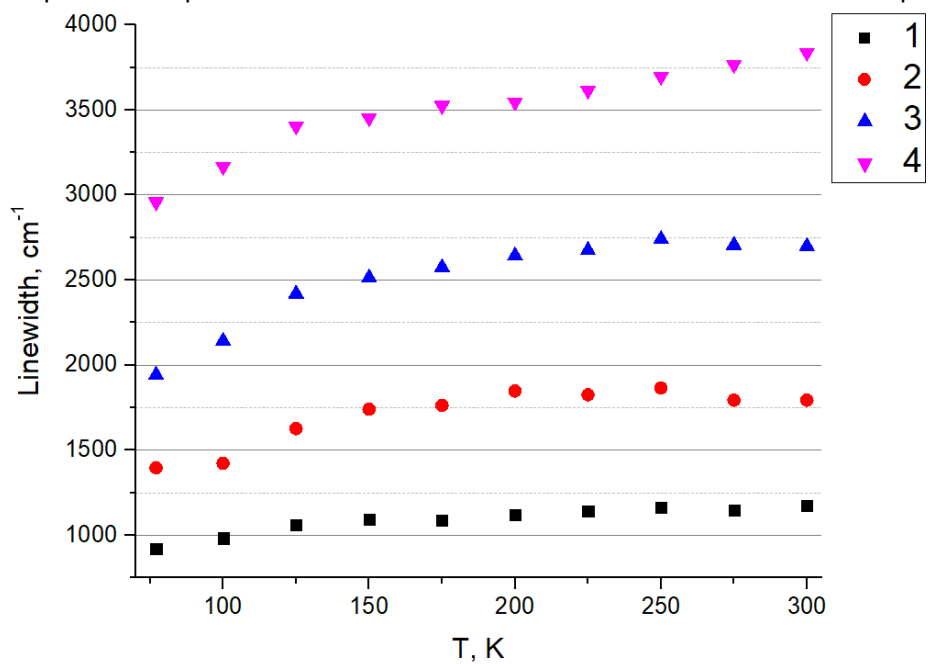
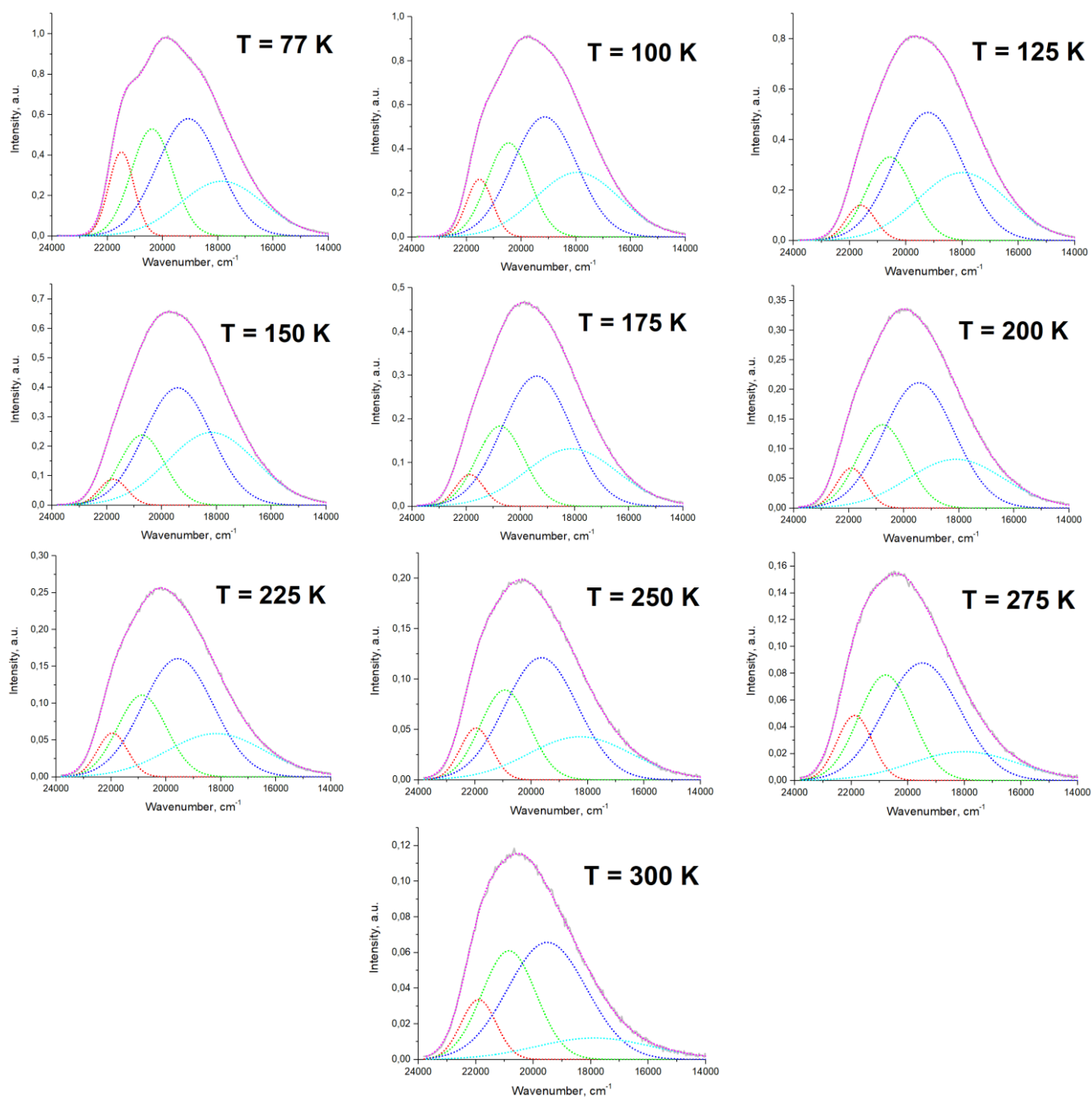


Figure S11. Temperature dependence of the linewidth of the Gauss functions for the complex  $[\text{Cu}_2\text{L}^1\text{I}_2]_n$ .

Table S31. The emission spectra of the complex  $[\text{Cu}_2\text{L}^2\text{I}_2]_n$  at  $T = 77\text{--}300\text{ K}$  resolved into four Gauss functions.





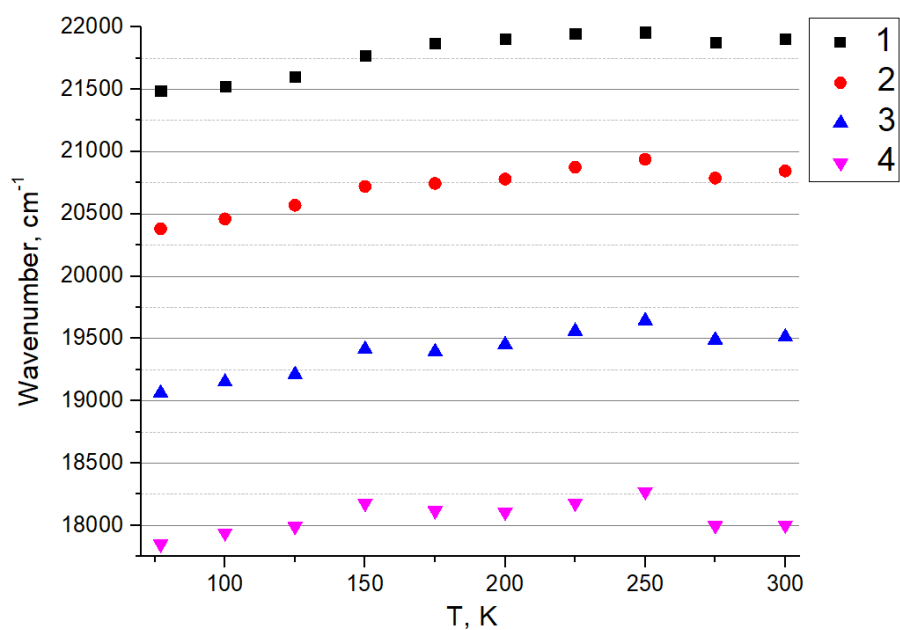


Figure S12. Temperature dependence of the maxima of the Gauss functions for the complex  $[\text{Cu}_2\text{L}^2\text{I}_2]_n$ .

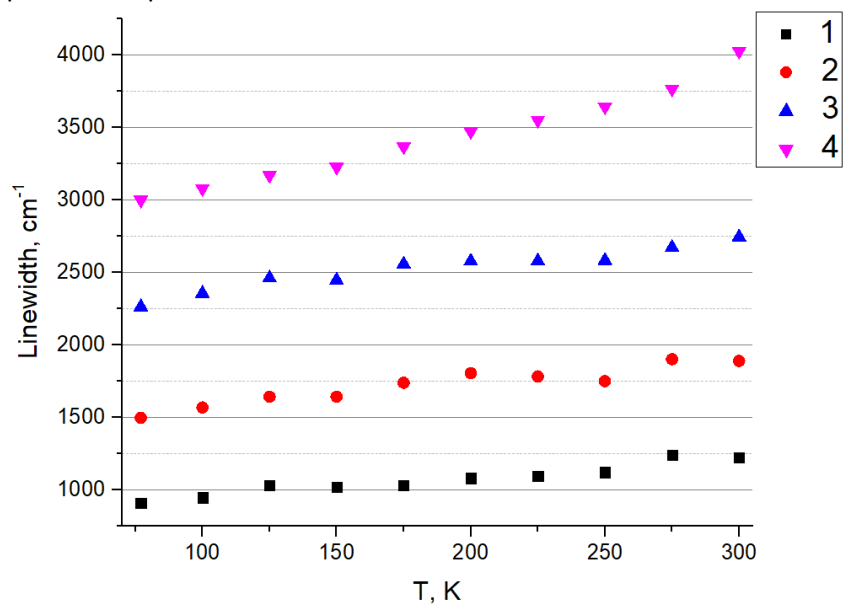
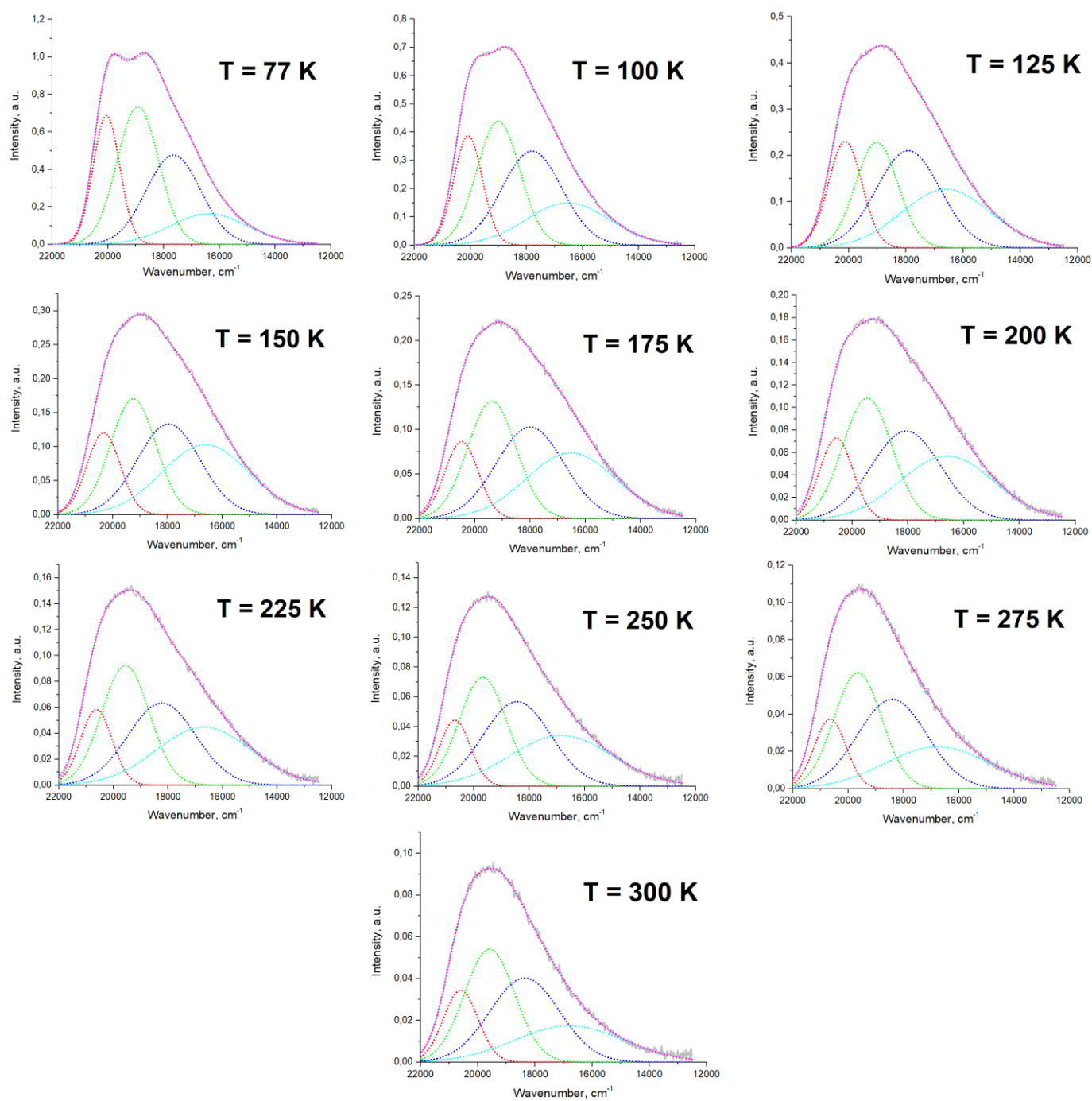


Figure S13. Temperature dependence of the linewidth of the Gauss functions for the complex  $[\text{Cu}_2\text{L}^2\text{I}_2]_n$ .

Table S32. The emission spectra of the complex  $[\text{CuL}^2\text{I}]_n$  at  $T = 77\text{--}300\text{ K}$  resolved into four Gauss functions.



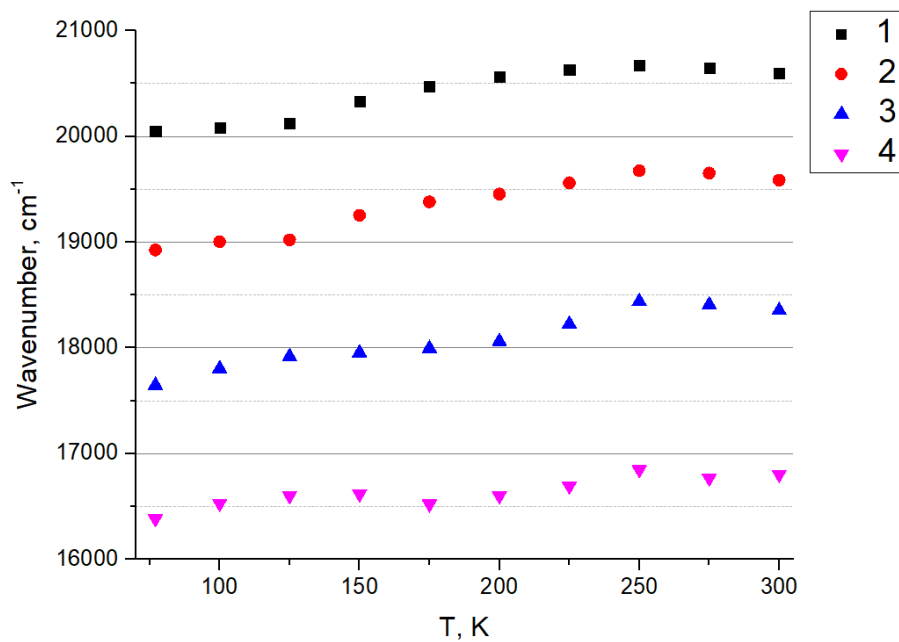


Figure S14. Temperature dependence of the maxima of the Gauss functions for the complex  $[\text{CuL}^2\text{I}]_n$ .

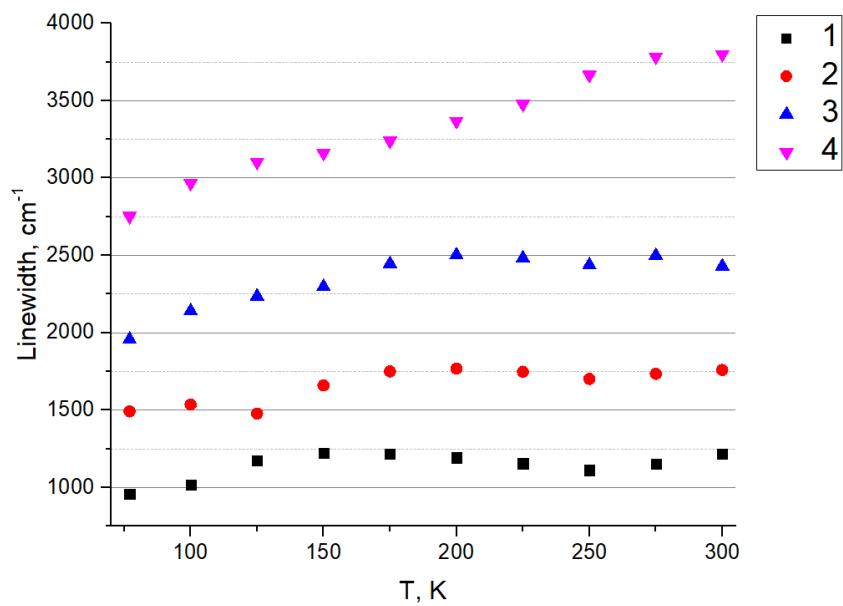


Figure S15. Temperature dependence of the linewidth of the Gauss functions for the complex  $[\text{CuL}^2\text{I}]_n$ .

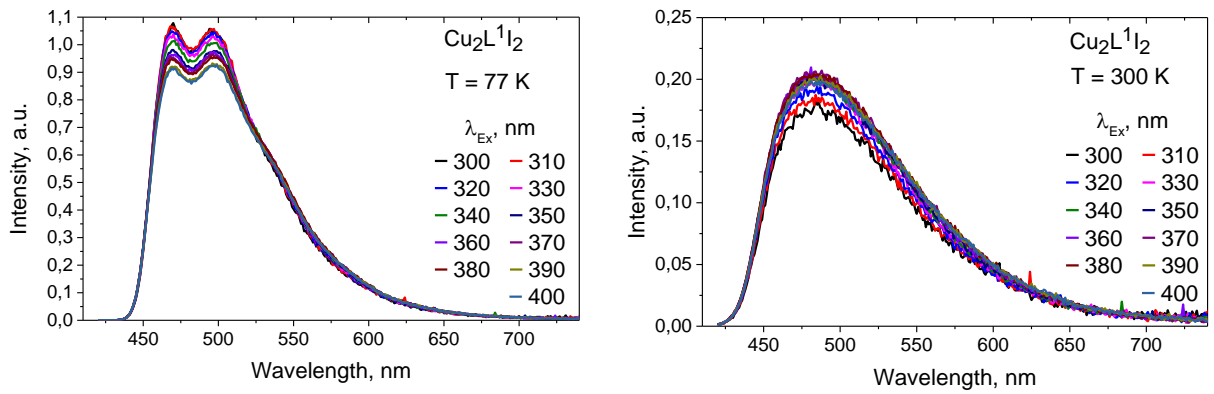


Figure S16. Dependence of the photoluminescence of the complex  $[\text{Cu}_2\text{L}^1\text{I}_2]_n$  on the excitation wavelength.

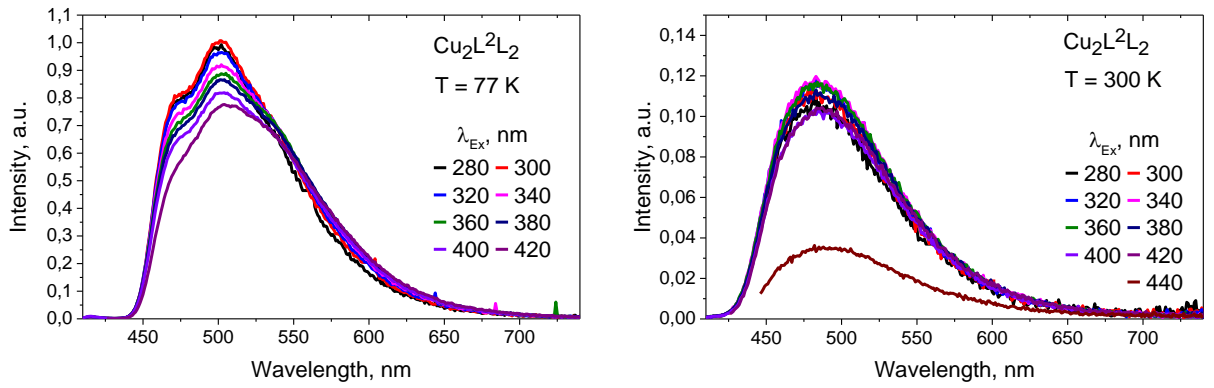


Figure S17. Dependence of the photoluminescence of the complex  $[\text{Cu}_2\text{L}^2\text{I}_2]_n$  on the excitation wavelength.

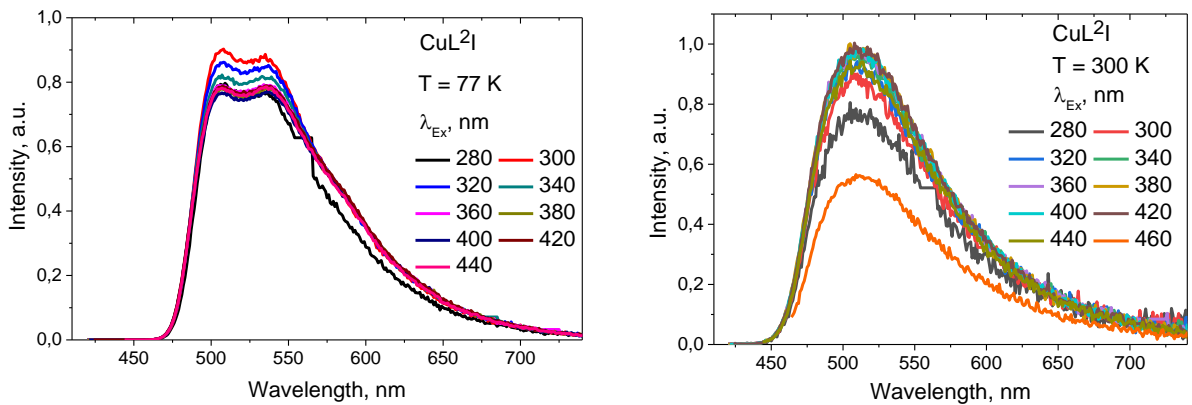


Figure S18. Dependence of the photoluminescence of the complex  $[\text{CuL}^2\text{I}]_n$  on the excitation wavelength.

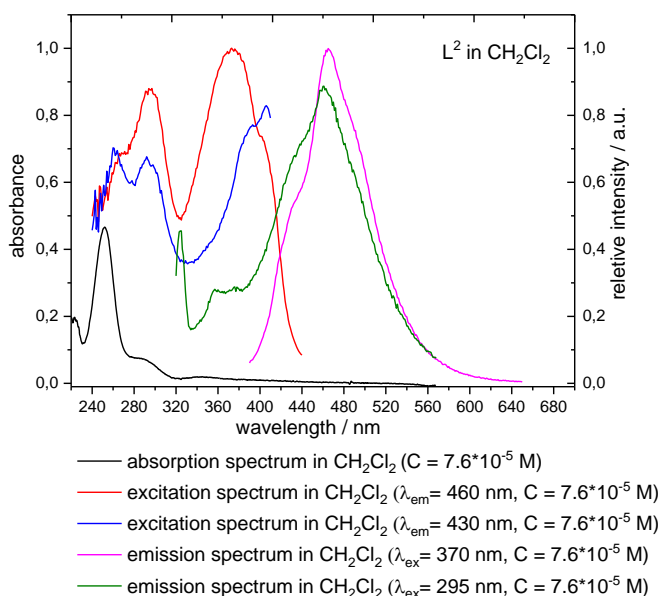
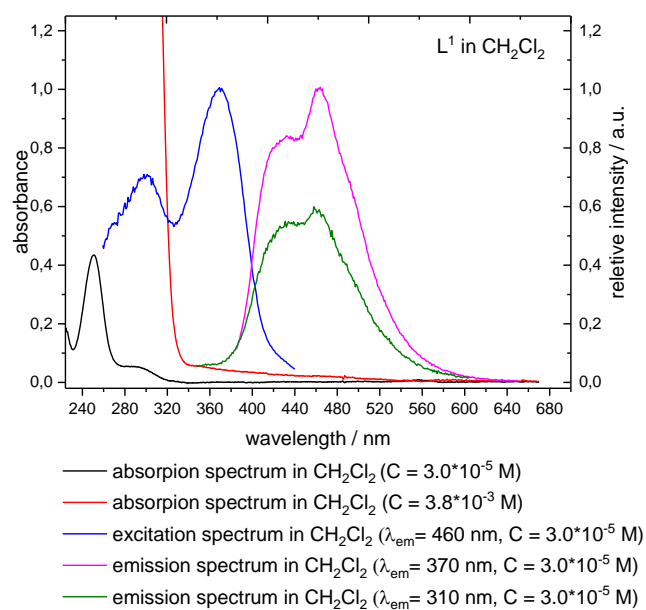


Figure S19. Absorption, excitation and emission spectra of  $\text{L}^1$  and  $\text{L}^2$  in  $\text{CH}_2\text{Cl}_2$ .

Free ligands in  $\text{CH}_2\text{Cl}_2$  solutions absorb at *ca.* 255, 290 and 360 nm (a weak absorption band). In the excitation spectra there are two bands near 300 nm and 370 nm. The ligands luminesce in the blue region of the spectrum with the maximum near 470 nm and a shoulder in the 400 – 440 nm range.

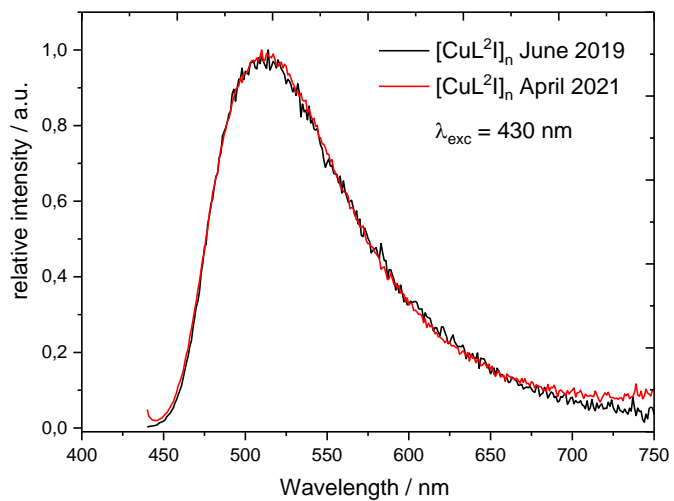
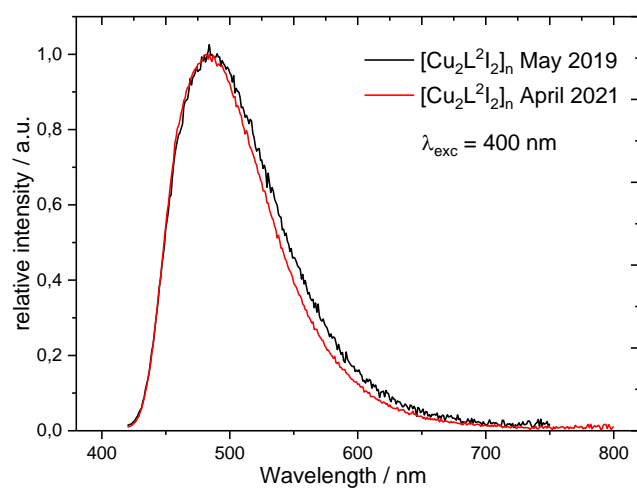
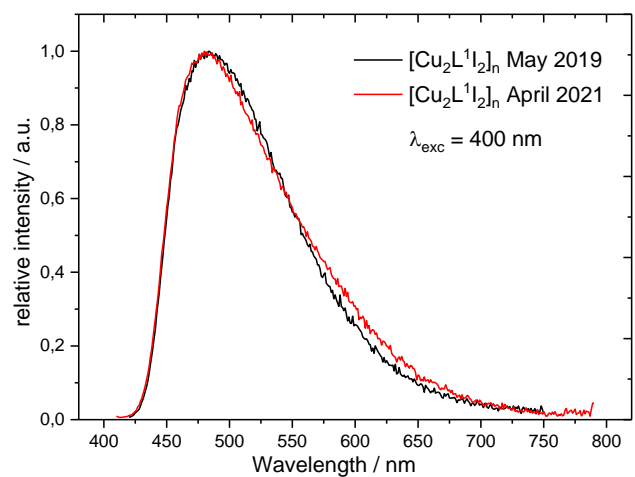


Figure S20. Reproducibility of emission spectra of the complexes.

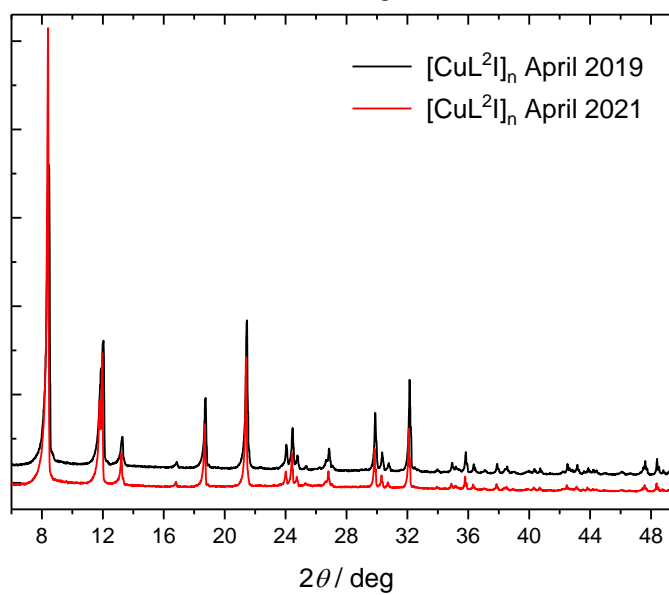
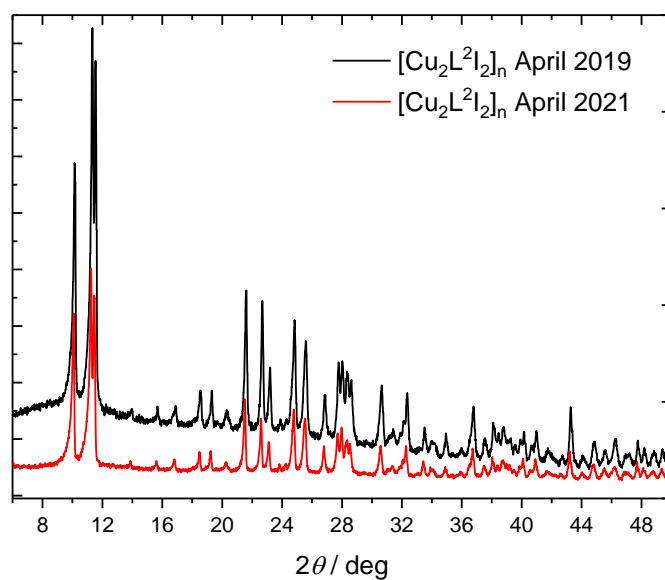
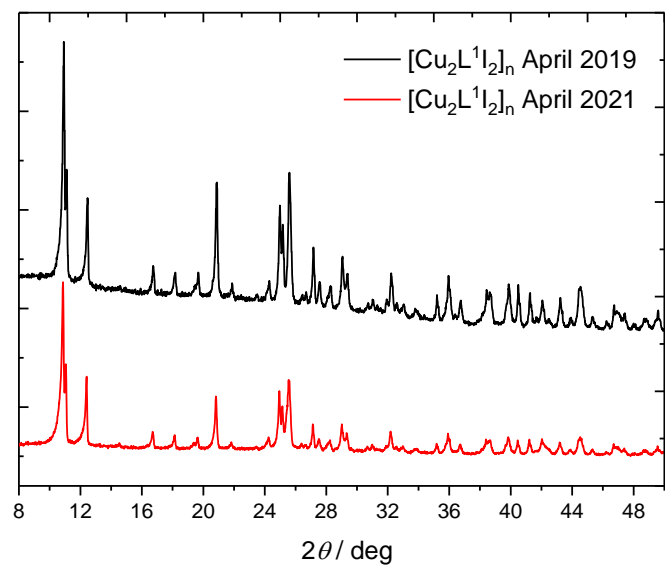


Figure S21. Reproducibility of X-ray powder diffraction patterns of the complexes.

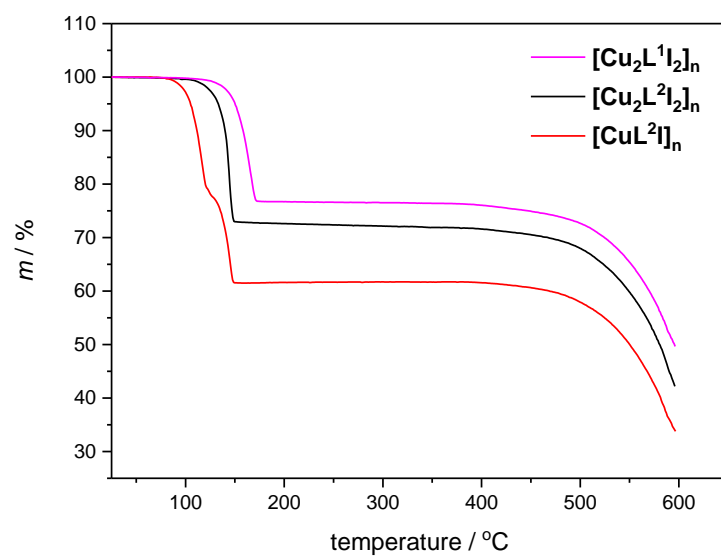


Figure S22. TGA data for the complexes.